New derivatives of urea-grafted alginate for improving the sorption of mercury ions in aqueous solutions

Benettayeb A, Morsli A, Guibal Eric, Kessas R

Materials Research Express

PAPER • OPEN ACCESS

New derivatives of urea-grafted alginate for improving the sorption of mercury ions in aqueous solutions

Materials Research Express

PAPER

New derivatives of urea-grafted alginate for improving the sorption of mercury ions in aqueous solutions

Benettayeb A[1,2,*], **Morsli A**[1,3], **Guibal E**[2,*] **and Kessas R**[1,4]

[1] Laboratoire de Génie Chimique et de catalyse hétérogène, Université de Sciences et de la Technologie, département de Génie Chimique - Mohamed Boudiaf, BP 1505 EL-M'NAOUAR, Oran, Algérie
[2] Polymer Composite and Hybrids, PCH, Institut Mines Telecom—Mines Ales, F-30319 Alès cedex, France
[3] Laboratoire de Chimie des Matériaux- Université d'Oran Ahmed Ben Bella, Oran, Algérie
[4] Pr. Rachid is deceased.
[*] Authors to whom any correspondence should be addressed.

E-mail: eric.guibal@mines-ales.fr **and** asmaa.benettayeb@univ-usto.dz

Keywords: mercury recovery, chemically-modified alginate beads, urea-grafting, sorption isotherms, uptake kinetics, multi-metal coexistenc

Supplementary material for this article is available online

OPEN ACCESS

RECEIVED
27 June 2020

REVISED
26 February 2021

ACCEPTED FOR PUBLICATION
1 March 2021

PUBLISHED
10 March 2021

Abstract

Chemically-modified alginate *(obtained by grafting urea on alginate, with different ratios; alginate-urea (1:1) and its new derivatives alginate-urea (1:2) with an exceed of the percent of amino group by 7%)* was successfully tested for mercury sorption in aqueous solutions. The influence of pH on metal sorption was first investigated: optimum pH was close to 5.5. Sorption isotherms were modeled using the Langmuir and the Sips equations, and sorption capacity slightly increased with the increased of the % of–NH_2 in the sorbent and the maximum sorption capacity exceeded 200 mg Hg l^{-1} (1.07 mmol Hg g^{-1}; for alginate-urea (1:2)), this means two times the sorption capacity of reference material (i.e., non-modified alginate), and also has a capacity improved compared to alginate-urea (1:1). Under selected experimental conditions the equilibrium was reached with 6–8 h of contact and the kinetic profiles were modeled using the pseudo-first order equation (PFORE), the pseudo-second-order rate equation (PSORE) and the resistance to intraparticle diffusion (RIDE). Surface functional groups, notably; –NH_2, –OH and –COOH, were involved in mercury sorption by alginate-urea, suggesting the ion exchange, complexation and/or electrostatic interaction of Hg(II) on the alginate-urea surface. The use of this material, environmentally friendly and simply obtained from a renewable resource, reveals promising for the treatment of low-metal concentration effluents: sorption capacities are comparable to alternative academic and commercials sorbents.

1. Introduction

The bioaccumulation of metal ions in the food chain, their intrinsic toxicity for human and animal beings *(with many health damages such as effects on nervous system, reproductive functions, skin, liver, etc)* are the main reasons that can explain the increasingly strict recommendations on the discharge of industrial and domestic effluents. International regulations are thus requiring the progressive decrease of contaminant levels in both discharged effluents and drinking water systems. Apart this environmental and regulatory incentive, the requirements imposed by several countries for the recycling of strategic, precious and highly-demanded metal ions are also driving a greater attention on the development of new processes for the competitive recovery of metal ions from diluted solutions. A wide spectrum of processes exists for the recovery of metal ions from aqueous effluents, depending on managed flows, levels of concentration and market value of these metal resources. Processes such as precipitation are frequently reported; however, the technical limitations (associated to the levels of residual concentration in function of the complexity of the solutions and presence of ligands), the poor selectivity that limits further metal valorization, and the production of huge amounts of contaminated sludge considerably

Table 1. Maximum acceptable level of mercury ions in drinking water in different countries ($\mu g\,l^{-1}$).

WHO	E.U.	U.S.	Canada	Australia	Japan	China
6	1	2	1	1	0.5	1

limit the potential application of this technique. Solvent extraction is commonly used for metal recovery from concentrated solutions [1], but fails to be competitive when the metal value is not high enough, when the flow rates are important and the concentration levels below 400–600 $mg\,l^{-1}$. Membranes processes [2] and electrochemical techniques [3] are also poorly competitive for complex systems For dilute solutions, below 200 $mg\,l^{-1}$, sorption processes represent efficient alternatives. The offer for sorbent materials is very large with chelating and ion-exchange resins [4–7], extractant impregnated resins [8], minerals [9–12], carbon-based materials [13, 14] etc. Biosorption has received a great attention for the last decades, using agriculture waste [15, 16], residues from fisheries, marine resources [17], etc. Biosorbents are processing through similar mechanisms to those involved in sorption processes: the functional groups at their surface, which are similar to those present on synthetic resins, may bind metal ions though chelation and ion-exchange mechanisms. These materials can be used in their raw form but many studies have also described the use of modified biopolymer-based sorbents, playing with the dual physical and chemical versatility of these materials. Indeed, it is relatively easy preparing hydrogels as spherical beads [18], foams [19], membranes [20, 21] etc. The presence of hydroxyl and/or amine groups on alginate and chitosan makes also the material easy to chemically modify by grafting new reactive groups [22–25].

Algal biomass, widely available, is used for the extraction of alginate and as a food ingredient; this biosorbent has intrinsic affinity for metal ions [26, 27], due to the presence of biopolymers such as alginate [28–31], carrageenan [32], fucoidan [33] that bear carboxylic, sulfonic groups, respectively. The levels of metal ions in the algal biomass should be strictly controlled for applications in food industry [34]. Alginate has been widely investigated since the 90's for its interaction with metal ions [35]. The biopolymer is mainly constituted of guluronic and mannuronic acid units (i.e., carboxylic group-bearing units), these acid groups are the main reactive groups that are involved in metal binding [36, 37] that can bind metal cations through ion-exchange and chelation. This mechanism is also responsible for the ionotropic gelation mechanism that is frequently used for preparing alginate gels. Through many metal ions can be used (mainly divalent cations, but trivalent cations can be also used), calcium is frequently preferred for preparing spherical beads. The hydrogels are especially stable in moderate acidic solutions and neutral solutions when the divalent cations contribute to stabilize the gel. Indeed, in the presence of sodium or potassium the gelation process may be reversed; this may limit their use in sodium- or potassium rich solutions. The sorption properties of alginate can be substantially improved by chemical modification. Recently, the grafting of urea on alginate was used for enhancing the sorption of Cu(II), Cd(II) and Pb(II) [38], and Ni(II), Zn(II) [39].

The present study focuses on the recovery of mercury, which is an emblematic example of highly-accumulative metal contaminant, this metal is recognized as one of the most toxic heavy metal pollutants in the aquatic environment due to its persistence and non-biodegradability [40]. The entry of mercury into food chain has been an alarming threat. The mercury ions can be transformed into methylmercury by micro-organisms [41]. The problem is perfectly illustrated by the '*Minamata disaster*': the uncontrolled release of industrial effluents in the ocean, the accumulation of the Mercury in the food chain and the fish-intake by local populations caused important neurological diseases to fisherman families. The availability of freshwater is an important issue for human health and social development [42]. Due to the low vapor pressure, inhalation is the main route of Hg(II) toxicity, which can cause death. Hg(II) lethal dose is defined between 150 and 300 mg/70 kg [43–45].

As shown in table 1, the maximum allowable concentrations of the Mercury in drinking water have been strictly set by the WHO and many countries [46]. This low concentration required in global standards, shows the importance of mercury treatment by bioadsorbents such as 'alginate-based materials' that are friends to the environment. Also shows the importance of testing the efficiency of treatment of low metallic concentrations. According to rule of Hard & Soft Acid-Base theory and the classification of Nieboer and Richardson, heavy metals can be classified into three categories and the Hg(II) belongs to class B which have an affinity towards the molecules of the center –N and –S of the same affinity, this metal is considered a soft Lewis acids of class B of strong polarizability. The advantage of this classification is that it makes it possible to predict potential metal binding sites within adsorbents and to foresee for each metal the best adsorbent and the best modification necessary. E. Guibal *et al* (2011),confirmed that the resultants of FT-IR analysis and the HASB rule confirmed that the nitrogen and sulfur atoms have an important role in Hg(II) adsorption [47]. Other researchers have confirmed the special importance of group –N in adsorption of mercury that it has a smaller effective ionic

radius than a plenty of metal ions in aqueous solution. And confirming that the Mercury ions Hg(II) ion shows a strong binding tendency to -N atom in functional groups, while N-containing compounds are also the preferred modifier for developing heavy metal adsorbents [48, 49]. There are researchers confirming that the main adsorption sites for Hg(II) ion are the –N and –O atoms because they have several lone pairs of electrons that can efficiently bind a metal ion to form a metal complex [50].

The advantage of choosing amine groups for the modification of the alginate is the low cost of modification with urea, biuret also the introduction of new functional groups by the simple way, also the literature is rich of modification of chitosan with amines –S containing such as cysteine which introduced thiol –SH functions which are also known by their high affinity towards Hg(II) [25].It is true that this functional group is known by their great affinity towards this metal (although chitosan likes mercury and forms stable bonds and sorption of almost 100% in the natural state [51, 52]) but the modification effected by most researchers to successfully graft such functions to the structure of chitosan is too expensive. There are researchers confirming that the main adsorption sites for Hg(II) ion are the –N and –O atoms because they have several lone pairs of electrons that can efficiently bind a metal ion to form a metal complex. According of these researchers the reason of these preference is that soft acid of Hg(II) ion offers high affinity toward soft bases of –C=O and C–CO–C groups and middle-soft bases of –NH–, –N=, and $–NH_2$ groups [50].

But despite these classification there remains the behavior of these unexpected biosorbents. So, just the preference of the center are predict but the positive way of modification and the cost remains estimating by each researcher. And depending on the type of biosorbent, the cost of water treatment per million liters of water was estimated as US $10–US $200, which presents biosorption as a cheap process compared to other known water treatment processes [53].

In this study, the biosorption properties of alginate and its modified forms (obtained by grafting different amounts of urea; Alginate-urea(1:1) and Alginate-urea(1:2)) are compared for Hg(II) recovery. The effect of pH is investigated before discussing uptake kinetics and sorption isotherms. The effect of competitor ions is also documented. The structure of the material is characterized by environmental scanning electron microscopy (ESEM), while ESEM-EDX (ESEM coupled with the energy dispersive x-ray analysis), pH-drift analysis (for determination of pH_{ZPC}, point of zero charge) and FTIR spectroscopy (Fourier-transform infra-red spectroscopy) are used for characterizing the sorbents and their interaction with metal ions.

2. Materials and Methods

2.1. Materials

Sodium alginate was supplied by FMC (La Madeleine, France). The commercial reference is LF-240D: this is a medium viscosity sample (11.5 mPa.s). The fractions of guluronic acid (G) and mannuronic acid (M) were quantified using the method described by Agulhon *et al* [54]: the G/M ratio was 0.33/0.67.

Urea (>99.0%) was purchased from Sigma-Aldrich (Taufkirchen, Germany). All the reagents used were of analytical grade, deionized water (Milli-Q Millipore) was systematically used for the preparation of solutions. Calcium chloride (>99.5%) was supplied by Chem-Lab (Chem-Lab NV, Zedelgem, Belgium). The mercury standard solution (C: 1 g Hg l^{-1}) was purchased from Carlo Erba France (Val de Reuil, France). The stock solution (at the concentration of 1 g l^{-1}) was prepared by dissolving of $HgCl_2$ salt (Carlo Erba) in HCl –acidified water. Solutions were prepared by dilution of the stock solution, just prior the experiment. The pH of the solution was controlled using 0.1 and 1.0 M HCl or NaOH solutions. The pH measurements were performed on a CyberScan pH 6000 pH-meter (Eutech Instruments, Nijkerk, The Netherlands).

2.2. Preparation of sorbents

The synthesis of the alginate-urea(1:1) sorbents was already described [38], in the preparation of alginate-urea (1:2) the mass of urea was increasing in order to test the capacity of the new material and its contribution to mercury adsorption. Briefly, solutions of 3.6% (w/v) of sodium alginate were prepared by mixing 3 g of biopolymer powder with 84 ml of Milli-Q water, for the reference alginate sorbent. For modified biopolymer, 1.116 g and 2.232 g of urea were added to the alginate solution for preparing the two derivatives: Alginate-urea (1:1) and alginate-urea(1:2), respectively. The reaction was processed under reflux at 50 °C for 3 h. The viscous solution was finally pumped, using a peristaltic pump, through a 0.8 mm gauge nozzle into 300 ml of a 0.2 M $CaCl_2$ solution. The beads formed during the ionotropic gelation were maintained overnight, under mild agitation, in the gelation solution. The beads were abundantly washed with Milli-Q prior to be used to remove calcium excess. A part of the stock was dried at 60 °C until weight stabilization, to evaluate the water fraction in the beads (f_w, %).

2.3. Characterization of materials

The morphological observation was performed using an environmental scanning electron microscope (ESEM) (Quanta FEG 200, FEI France, Thermo Fisher Scientific, Mérignac, France). The composition of the beads was semi-quantitatively analyzed using ESEM-EDX, ESEM coupled with an energy dispersive x-ray microanalyzer (Oxford Instruments France, Saclay, France).

The chemical reactive groups have been identified using FTIR spectrometry (Fourier-Transform infra-red spectrometry) using a Bruker VERTEX70 spectrometer (Bruker Optic GmbH, Ettlingen, Germany) equipped with an ATR tool (attenuated total reflectance).

The amine content in the sorbent was estimated using a volumetric method [55–57]: 50 ml of 0.2 M HCl solution was added to 0.005 g of sorbent under agitation for 15 h. The residual concentration of HCl was estimated through titration against 0.2 M NaOH solution using phenolphthalein as the indicator. The number of moles of HCl having interacted with amino groups and consequently the amino group concentration (mmol —NH g^{-1}) was calculated from equation (1):

$$\text{Concentration of amino group} = (M_1\text{-}M_2) \times 50/0.005 \quad (1)$$

where; M_1 and M_2 are the initial and final concentrations of HCl, respectively.

The point of zero charge (pH_{pzc}) of the adsorbent was determined using the method described by Lopez-Ramon *et al* [58]. A fixed amount of sorbent (i.e., 125 mg) was mixed at room temperature with 125 ml of 0.1 M NaCl solutions at fixed values of pH_0 ranging between 2.0 and 12.0. After 48 h of contact, the equilibrium pH_{eq} was measured and plotted against pH_0; the pH_{PZC} corresponds to the pH value where $pH_0 = pH_{eq}$.

2.4. Sorption tests

The experiments were performed by mixing a fixed amount of beads (m, g, the dry amount of alginate-based material was determined by correction of the wet volume with the fraction of water, f_w) with a constant volume of solution (V, L). The pH_0 was varied for the study of pH effect and set to 5.5 for the study of other experimental parameters. The pH was not adjusted during the sorption, but the pH was systematically monitored at the end of the experiments (pH_{eq}). After 8 h of contact under agitation (v: 150 rpm), the solution was filtrated using 1 μm-size pore membranes and the residual concentration (C_{eq}, mg Hg l^{-1} or mmol Hg l^{-1}) was determined by ICP-AES (inductively-coupled plasma atomic emission spectroscopy, Horiba Jobin-Yvon Activa M, Longjumeau, France). The sorption efficiency (SE, %) was calculated ($SE=(C_0 - C_{eq})^*100/C_0$) and the sorption capacity (q_{eq}, mg Hg g^{-1} or mmol Hg g^{-1}) was determined using the mass balance equation: $q_{eq} = V(C_0 - C_{eq})/m$.

For the study of uptake kinetics, a wet mass of sorbent (m: 2.5 g, corresponding to 50 mg dry weight) was maintained under agitation (v: 150 rpm) for 8 h with a volume, V = 500 ml, of mercury solution (C_0: 10 or 50 mg Hg l^{-1}). Samples were collected at fixed contact times, filtrated using 1 μm-size pore membranes and the filtrate was analyzed for metal concentration using ICP-AES.

The initial metal concentration (C_0) was varied between 2 and 250 mg Hg l^{-1} (i.e., 0.01–1.25 mmol Hg l^{-1}) for investigating the sorption isotherm at pH 5.5. Fifty mg of wet beads (i.e., 1 mg dry weight) were mixed with 10 ml of each mercury solution. After 8 h of contact, the residual concentration in the filtrate was analyzed by ICP-AES and the sorption capacities were calculated for the different points, and plotted in function of residual concentration ($q_{eq} = f(C_{eq})$).

2.5. Modeling of sorption process and uptake kinetics

The study of mass transfer is important for determining the equilibrium time but also for identifying the limiting steps (and then orienting the required changes in the structure of the material for improving global performance). Sorption kinetics [59] may be controlled by:

(a) the proper reaction rate, which can be approached by simple equations like the pseudo-first order rate equation (PFORE) [60], and the pseudo-second order rate equation (PSORE) [61]. These equations, initially developed for the modeling of homogeneous chemical reaction, are frequently used for heterogeneous systems, like sorption processes. In this case, the occurrence of diffusion limitations induces that the rate parameters should be considered as apparent rate parameters.

(b) different mechanisms of resistance to diffusion, such as bulk diffusion, film diffusion and intraparticle diffusion [62]. The resistance to bulk diffusion is generally negligible when the suspension is efficiently agitated (preventing the heterogeneous dispersion of the sorbent), while the effect of resistance to film diffusion is mainly limited to the very first minutes of contact, especially when the agitation is weak (i.e., 100 rpm or below). In most cases, for the whole range of contact time, the resistance to intraparticle diffusion is playing the major controlling role. Sophisticated models exist that take into account the different mechanisms but they require complex numerical analysis and complete characterization of the

Table 2. Characteristics and physical properties of gel beads.

Properties	Alginate	Alginate-urea(1:1)	Alginate-urea(1:2)
Average bead diameter (mm)	2.5	2.5	2.5
Wet weight per bead (mg)	10 ± 0.5	12.5 ± 0.5	12.5 ± 0.9
Dry weight per bead (mg)	0.2 ± 0.5	0.25 ± 0.5	0.25 ± 0.9
Water content (%)	98.0 ± 0.8	98.0 ± 0.9	97.0 ± 0.7
% amino group	—	12.14	17.63
pH_{ZPC}	5.04	6.78	7.13

materials in terms of morphology, and textural properties [59, 63]. In a first approach, it is possible using a simplified and independent modeling based on the Crank equation [64]. A reminder of these equations is reported in the Additional Material section (section 2, Eq. AM1-3).

The sorption isotherms represent the distribution of the solute between solid and liquid phases at equilibrium and under constant temperature. Three models were used for analyzing sorption isotherms (a) the Langmuir equation [65, 66], the Temkin equation [67, 68], and the Sips equation, also called Langmuir-Freundlich equation [69–71], which are described by Eq. AM4-7, respectively (see Additional Material section, section 3).

3. Results and discussion

3.1. Characterization of materials

3.1.1. Titration and determination of pH_{ZPC}

Figure AM1 (available online at stacks.iop.org/MRX/8/035303/mmedia) (see Additional Material section) shows the comparison of equilibrium and initial values of pH when applying the pH-drift method. The pH-profiles are very similar for the two urea-modified samples of alginate: the degree of substitution hardly affects the acid-base properties of the material. The pH_{ZPC} values are respectively 6.78 [38] and 7.13; this is about 1.7–2 pH-units higher than the value determined for the Alginate sample (i.e., $pH_{ZPC} = 5.04$). The pK_a values of acid and guluronic acid in alginate are reported close to 3.38 and 3.65, respectively [72]. The ΔpH is maximum (and positive) at pH 4 and tends to decrease till reaching a minimum (negative value) at pH close to 7 for alginate sorbent. At acidic pH the sorbent is protonated (predominance of carboxylic groups), while in mild-acidic conditions the cationic behavior decreases and the sorbent is progressively deprotonated and carboxylate groups predominate. For urea-modified alginate, the deprotonation frontier is shifted toward higher pH values (around pH 7); this may affect the electrostatic effects.

Table 2 reports some of the physical characteristics of sorbent hydrogels (average size of beads, water content, etc), which are hardly affected by the chemical modification of the material. In addition, the results obtained by acid-base titration are also reported and converted into nitrogen (i.e., amine group) content for urea-modified materials. The amine groups are quantified into Alginate-urea(1:1) and Alginate-urea(1:2) beads close to 8.67 mmol N g^{-1} (about 12.14%, w/w) and 12.59 mmol N g^{-1} (about 17.63%, w/w), respectively. The semi-quantitative analysis of Alginate-urea(1:1) by ESEM-EDX analysis confirms the order of magnitude in nitrogen content (close to 11.7%, w/w (not shown)).

3.1.2. FTIR spectroscopy

The interpretation of FTIR spectra of the sorbents was already discussed in a previous paper [38]. The main peaks assigned to uronic acids have been identified at the following wavenumbers: 970 cm^{-1}, 840 cm^{-1}, 1414 cm^{-1} (–C–OH bending vibration combined with O–C–O vibration), 1587 cm^{-1} (asymmetric stretching of carboxylate O–C–O vibration) for alginate. After urea grafting, the typical stretching vibration of primary amine groups is appearing at 1146 cm^{-1}; in addition, the grafting of urea is shifting several bands in the region 1300–1000 cm^{-1} [38]. The zone 1300–1000 cm^{-1} shows different peaks or shoulders characteristic of pyranose group: they are assigned to C–C–H and O–C–H bending modes (around 1300 cm^{-1}), C–O stretching (around 1147 cm^{-1}) and C–O and C–C stretching vibrations (around 1058 cm^{-1}).

The FTIR spectra of the Alginate-urea sorbents were characterized after mercury binding (figure 1). Hg(II)-loaded samples were obtained by contact of the sorbents at pH 5.5 for 8 h with sorbent dosage: 0.1 $g.l^{-1}$, and initial metal concentration, C_0: 10 mg Hg l^{-1}(i.e., 0.05 mmol Hg l^{-1}). Changing the amount of urea grafted on alginate hardly affects FTIR spectra; the only difference is observed in the shift of some of the FTIR bands. After urea grafting two strong peaks appeared at 3500–3400 and 3380–3300 cm^{-1} which are assigned to two N-H stretching vibrations (out-of-phase and in-phase, respectively) [38]. After mercury binding, these peaks are

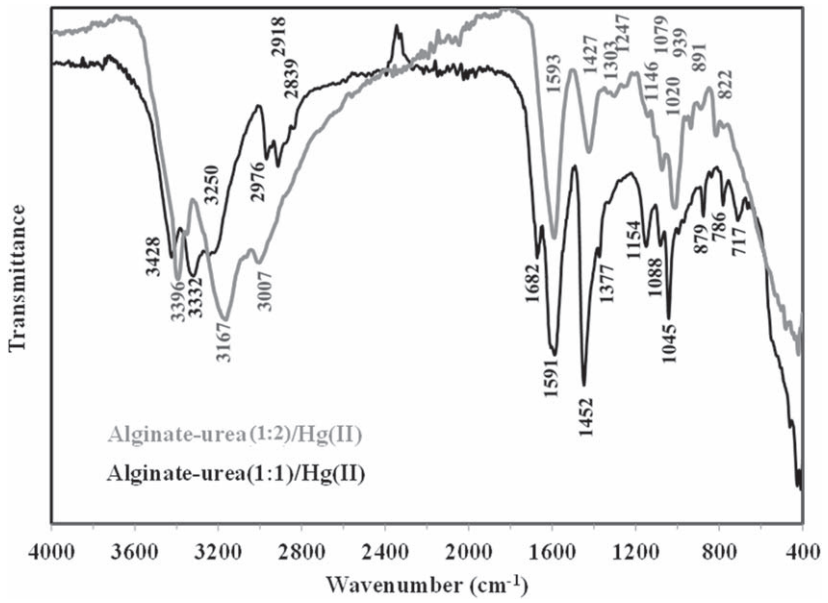

Figure 1. FTIR spectra of sorbents (Alginate-urea (1:1) and Alginate-urea (1:2)) after Hg(II) sorption.

shifted to 3428–3315 cm^{-1} in the case of Alginate-urea(1:1) and 3394–3160 cm^{-1} in the case of Alginate-urea (1:2). In addition, the width and intensity of this peak is considerably increased for Alginate-urea(1:2), consistently with the increase in nitrogen content (as determined by titration).

The series of –CH vibrations are reported around 2976, 2918 cm^{-1} (in the Alginate-urea (1:2)) and 3007 cm^{-1}(in the Alginate-urea(1:1)). After Hg(II) sorption on Alginate-urea (1:1) the most representative bands are identified at 1593 cm^{-1} (C–O stretching and $–NH_2$ scissoring), the band around 1427 cm^{-1} is attributed to C–N stretching vibration, Alginate-urea shows a band at 1146 cm^{-1} which is probably attributed to primary amine stretching vibration, while the strong peak at 1020 cm^{-1} may be assigned to the combination of several bands associated to C–O–C (pyranose unit), C–N stretching and C–O stretching vibrations.

For the Alginate-urea(1:2)-loaded Hg(II) material, bands are appearing at 1682 cm^{-1} (i.e., C=O and C–O and C–N stretching vibrations), at 1591 cm^{-1} (C–O stretching and NH_2 scissoring), the band around 1452 cm^{-1} is attributed to C–N stretching vibration. The intensities of the bands are stronger due to higher amine grafting. The bands are shifted after Hg(II) binding by comparison to the spectra of the sorbents prior to metal binding [38]. This confirms that carboxylic groups may be involved in metal binding but the presence of amine groups substantially increase metal binding because of the strong affinity of mercury ions for amine-based functional groups.

3.1.3. SEM and SEM-EDX analyses

Figure 2 shows the SEM observation of Alginate-urea (1:1) beads (morphology and surface aspect at different magnitudes) before and after metal sorption. The beads are roughly spherical with small deformations (probably explained to drying process). The drying process induces an irregular shrinking of the beads that causes the appearance of irregularities at the surface of the material (striations or ridges at low magnitude and smoothed hills and valleys at higher magnitude). The general morphology of the beads is not changed after mercury sorption. Figure 3 shows the ESEM-EDX analysis of these samples (i.e., before and after Hg(II) sorption). Metal sorption is confirmed by the appearance of the characteristic peaks of mercury, while the peak of sodium disappeared and the intensity of calcium decreases (semi-quantitative analysis obtained by ESEM-EDX, not shown).

It is noteworthy that the sorption of Hg(II) is significantly stronger onto the Alginate-urea(1:2) compared than into Alginate-urea(1:1) (not shown): the density of element is much strong intense; this will be confirmed by the comparison of sorption capacities (see below), that, we can conclude that the adsorption of mercury increases with the increase in the amount of the nitrogen groups due to the functionalization at two rations of Alginate-urea(1:1) and (1:2).

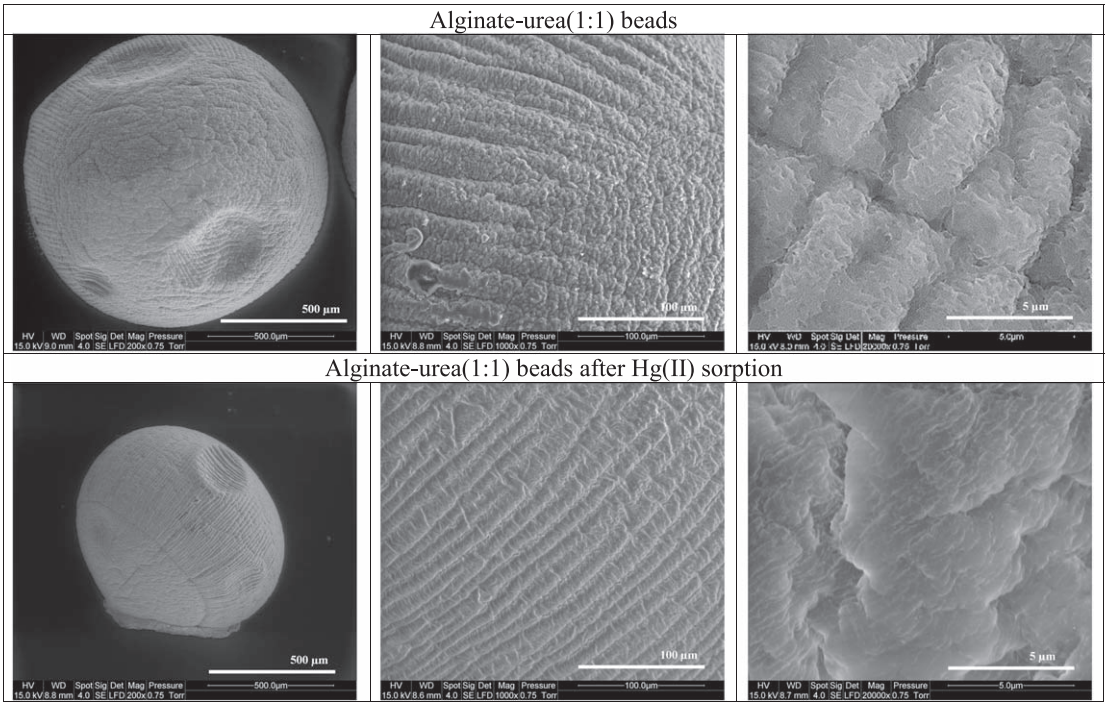

Figure 2. SEM micrographs of alginate beads (a); alginate-urea beads unloaded and Hg (II)-loaded alginate-urea beads (b) at (0.05 mmol $Hg.l^{-1}$), (the scale bars are 500, 100 and 5.0 nm, respectively).

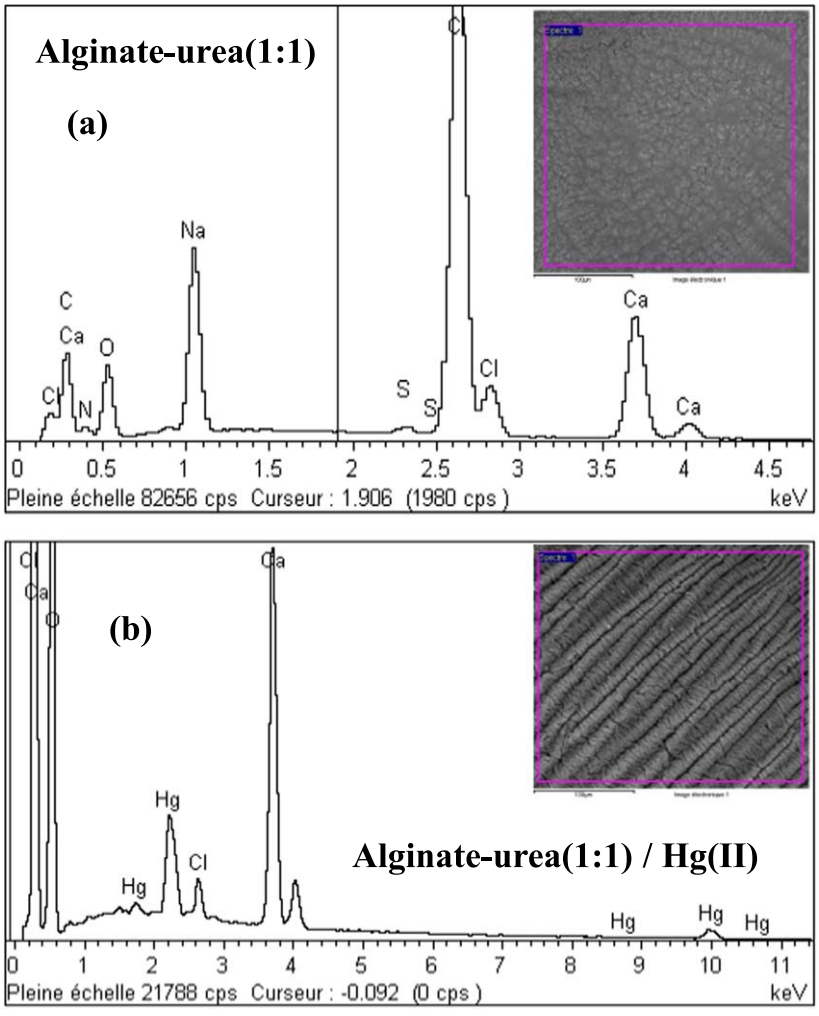

Figure 3. Energy dispersive X-ray analysis (EDX) of alginate-urea (1:1) beads before (a) and after (b) Hg(II) sorption.

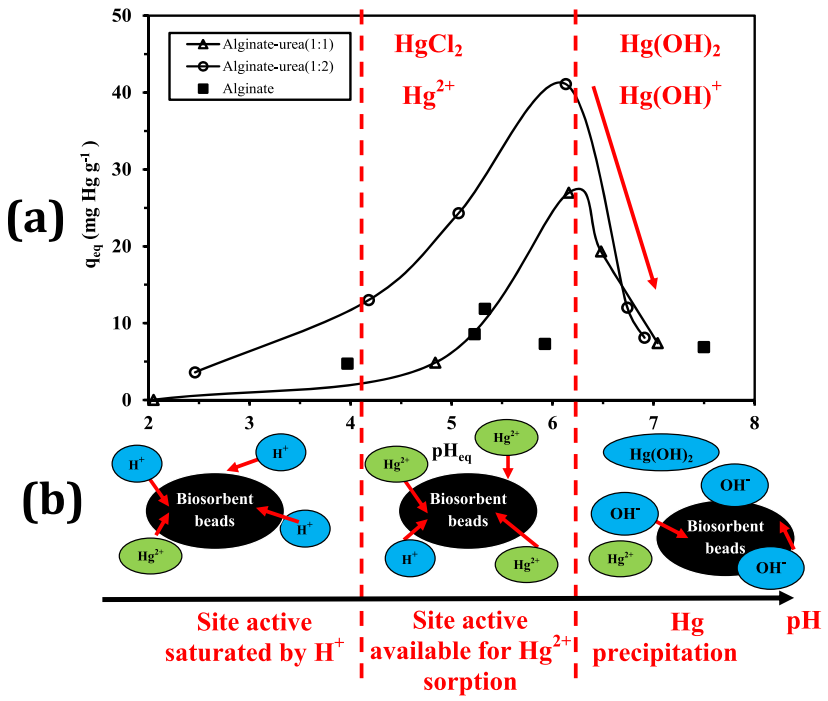

Figure 4. (a) Effect of pH on the removal efficiency of Alginate, Alginate-urea(1:1) and Alginate-urea(1:2) beads for Hg(II) ions (t = 8 h, T = 20 ± 1 °C, sorbent dosage; SD = 0.1 g.l^{-1}, C_0 = 0.25 mmol Hg l^{-1}; agitation speed (horizontal Shaker) 150 rpm), (b) competition between Hg and other spaces in solution in an active site at different pH values.

3.2. Effect of pH on metal sorption

The pH is a critical parameter for the design of a sorption process. Indeed, the pH may affect: (a) the chemical state of reactive groups (protonation/deprotonation) and then their affinity for metal ions (electrostatic attraction mechanism, competition effect of protons), and/or (b) the speciation of metal ions (especially in the presence of ligands) [73, 74].

Figure 4 compares the sorption capacity obtained for different pH values under similar experimental conditions for the reference material (i.e., Alginate beads) and for modified alginate sorbents (Alginate-urea (1:1) and Alginate-urea (1:2)). For Alginate beads, the pH hardly affected metal sorption between pH 4 and 7.5: the sorption capacity varied between 5 and 12 mg Hg g^{-1}. Above pH 4, carboxylic groups are progressively deprotonated making possible the binding of metal cations; however, sorbent affinity for mercury remains very low. After grafting urea (and amine groups) the sorption capacities significantly increased, due to the affinity of amine groups for Hg(II). However, the sorption capacity was strongly controlled by the pH. At pH close to 2, the two sorbents have very low sorption capacities due to the protonation of amine groups (and carboxylic groups); the repulsion of metal cations by protonated groups limits metal binding. While the pH increased the protonation of amine groups progressively decreased and metal sorption increased. A maximum in sorption capacity was reached closed to pH 6. It is noteworthy that above pH 6 the sorption capacity drastically reduced; although the pH_{ZPC} for the two sorbents were in the range 6.7–7. This means that the protonation of amine groups is not the sole parameter that controls metal binding on the sorbent. Actually, the calculation of metal speciation, under selected experimental conditions, using Visual Minteq software [75], shows that at pH 5 the predominating form of mercury ions is $HgCl_2$ (76%) completed with HgClOH (22%). When the pH increases the distribution of mercury species changes: at pH 6 (optimum pH value) $HgCl_2$ represents about 43% (against 47% for HgClOH and 10% for $Hg(OH)_2$) and at pH 7 $HgCl_2$ represents only 8.4% for 44% of HgClOH and 47% for $Hg(OH)_2$). The affinity of the sorbent for mercury decreases when the distribution of mercury is displaced toward the formation of hydrolyzed species. The effective sorption of mercury is then controlled by the simultaneous deprotonation of amine groups and the predominance of neutral mercury chloride species (against hydrolyzed species). The researchers have confirmed that below pH 6 $HgCl_2^0$ is the dominant Hg species. Other researchers have confirmed that below pH 6 the $HgCl_2^0$ is the dominant Hg species with a slight presence of $HgCl(OH)^0$ [76]. Arias *et al* (2017) confirming these results and found that $HgCl_2$ is the predominant species for pH values between 3.5 and 5.5, and Hg(OH)Cl or $HgCl_2^-$ are the predominant species when the pH is between 5.5 and 6.5, while at a pH greater than 6.5, $Hg(OH)_2$ or $HgCl_4^{2-}$ are the predominant species [77]. Also we remarked that at the pH value of 5.5 the efficacy of sorbents are better than other value and according to D.

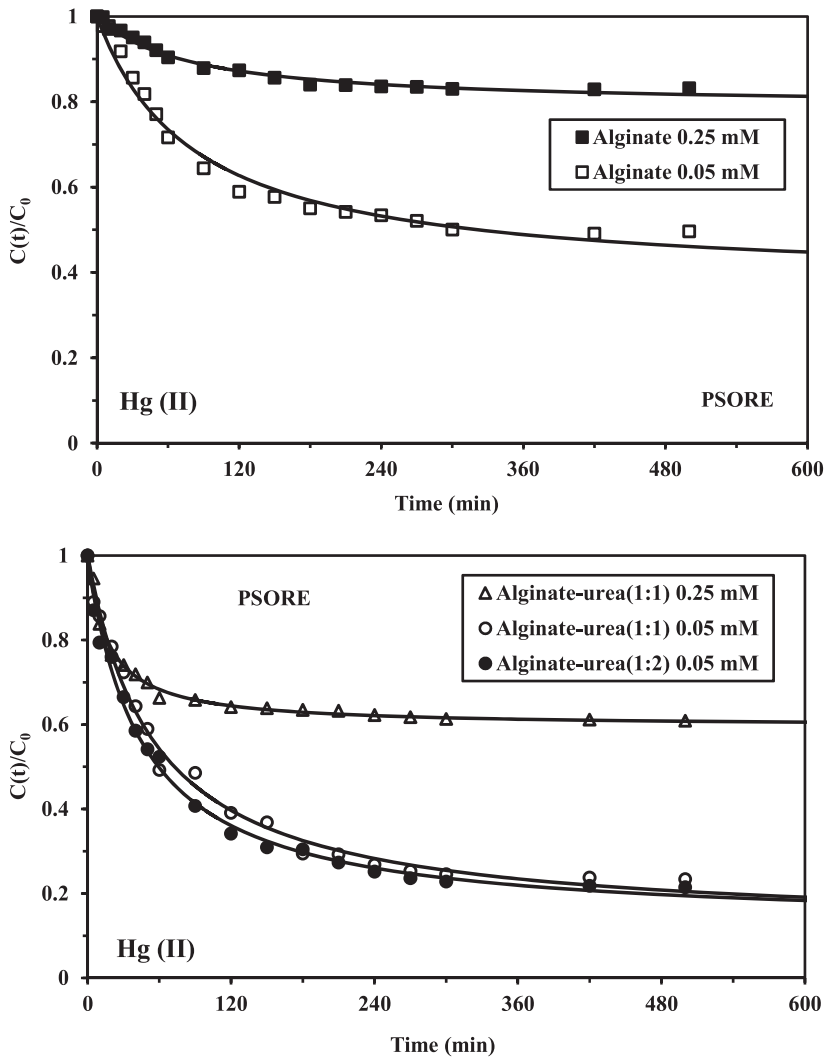

Figure 5. Hg(II) uptake kinetics on Alginate, Alginate-urea and Alginate-biuret beads (SD: 0.1 g (d.w.) l^{-1}; C_0:0.05 and 0.25 mM (10 and 50 mg Hg l^{-1})—mono-component solutions; T: 20°C; pH 5.5; solid-lines: modelling of the kinetic profile with the PSORE and parameters from table 4).

Zhang *et al* (2020) with the increase in pH value, protonation of amino groups becomes weaken, and their coordination ability with heavy metal ions increases [40].

Figure AM3 (see Additional Material section 1, for complementary information) shows the pH variation during mercury sorption: In most cases, the pH slightly increases and the variation remains below 0.5 pH unit. The pH variation, under selected experimental conditions (metal concentration, dose, T and t), was low enough to avoid metal precipitation. The profiles of pH variations are very similar for the two derivatives with an equilibrium value that is slightly higher than the initial pH value till pH 6; above pH 6 the equilibrium pH tended to decrease (probably due to the formation of hydrolyzed mercury species) or to the release of protons due to a diversity of reactions. Sonmez *et al* used grafted polyacrylamide chains for mercury binding and reported metal ion binding through the interaction of Hg(II) with amine groups on the acrylamide moiety [78]: R-(C=O)-NH-$Hg^{+}X^{-}$ or R-(C=O)-NH-Hg-NH-(C=O)-R, with proton release. In the case of alginate, equilibrium pH systematically remained below the initial pH by less than 0.5 pH unit; this is due to the deprotonation of carboxylic groups and the weak metal sorption does not significantly affect pH variation.

For further studies, the pH was set to pH 5.5 to prevent the possible phenomena of precipitation (at the highest metal concentration range, for example in the study of sorption isotherms) while preserving good pH conditions for metal sorption (associated to the predominance of neutral mercury chloride complexes).

3.3. Uptake kinetics

Figures 5 and 6 show the kinetic profiles for mercury sorption using Alginate beads as the reference material and modified alginate beads (i.e., Alginate-urea (1:1) and Alginate-urea (1:2)) for different experimental conditions.

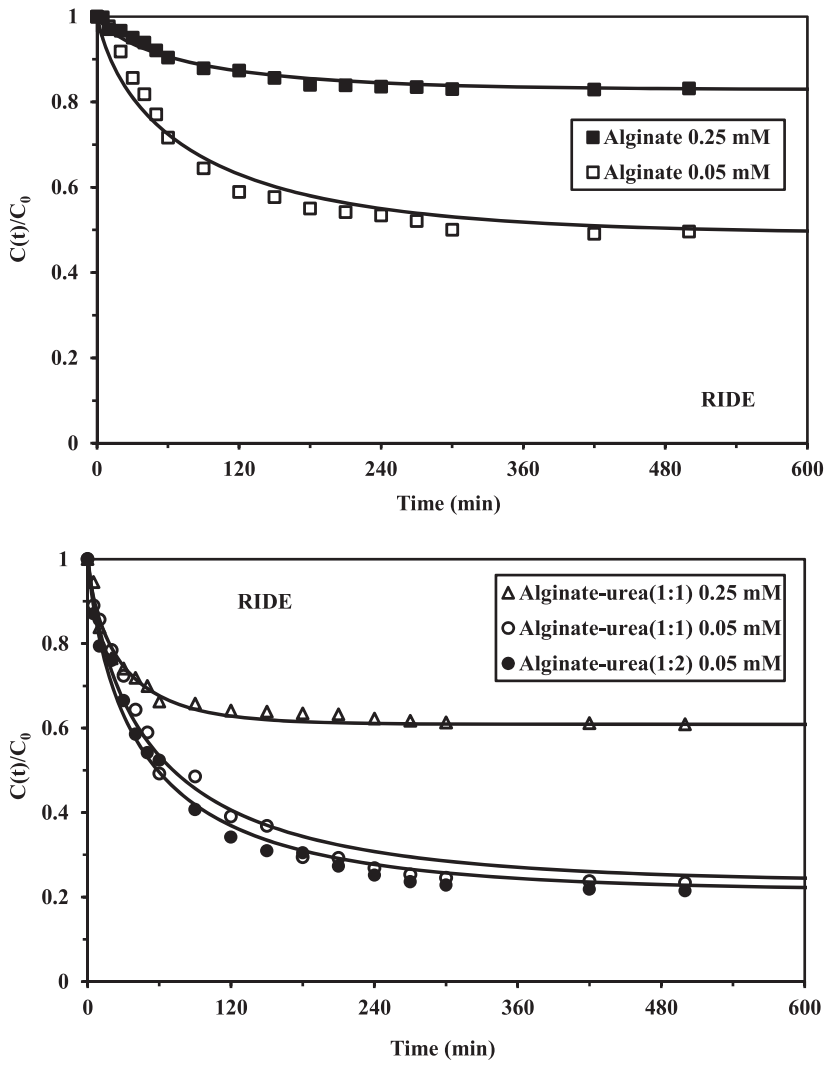

Figure 6. Hg(II) uptake kinetics on Alginate, Alginate-urea(1:1) and Alginate-urea(1:2) beads (SD: 0.1 g (d.w.) l^{-1}; C_0: 0.05 and 0.25 mM (10 and 50 mg Hg l^{-1})– mono-component solutions; T: 20°C; pH 5.5; 150 rpm; solid-lines: modelling of kinetic profile with the RIDE (Crank equation) and parameters from table 3).

Figure 6 shows the kinetic profiles fitted by the RIDE (resistance to intraparticle diffusion, the so-called Crank equation) while figure 5 shows the fits of experimental data using the PSORE. The preliminary observation of the kinetic profiles shows that with alginate materials a minimum of 8 h is necessary for approaching the equilibrium while for modified alginate the equilibrium was reached within 5 h. The modification of the sorbent not only increases sorption capacity but also mass transfer performance. Anyway, the uptake kinetics remains relatively slow; this confirms the relative importance of the mechanisms of resistance to intraparticle diffusion on the global control of uptake kinetics [79, 80]. It is noteworthy that the sorbents were used under their wet form (without being dried: the drying may cause the irreversible collapse of the porous structure, which, in turn, affects accessibility to reactive groups and mass transfer performance) [38, 81], and causes slow kinetics [38, 82]. Actually, the kinetic profiles can be described by a two-step profile: (a) a first initial section corresponding to 30–45 min and more than 50%–60% of total sorption), followed by (b) a much slower sorption phase that lasts for several hours. The first phase corresponds to the sorption at the external surface or within the first external layers of the alginate beads, while the second phase may be assigned to the diffusion of metal ions to the core of the beads.

The modeling of kinetic profiles with the RIDE and the PSORE gives relatively good fit of experimental data. Solid lines on figures 6 and 5 represent the fits with the RIDE and the PSORE, using the parameters reported in tables 3 and 4, respectively. A similar study was performed using the PFORE (see Additional Material section, section 2, figure AM4 and table AM1). Some discrepancies can be observed in the comparison of experimental sorption capacities at equilibrium and the fitted values for both PFORE and PSORE. Actually the superimposition of fitted curves for the three models with experimental profiles shows that all of them respect the kinetic trends. The intraparticle diffusion coefficients vary with the sorbent and mercury concentration; however, they are all in the same order of magnitude (1.7–8.2 $\times$ 10^{-9} m^2 min^{-1}) and much lower than the

Table 3. Modeling of uptake kinetics using the Crank equation (RIDE)—Mono-component solutions (SD: 0.1 g (d.w.) l^{-1}).

C_0 (mmol Hg l^{-1})	Sorbent	$D_e \times 10^9$ (m^2 min^{-1})	EV
0.05	Alginate	2.362	0.078
	Alginate-urea(1:1)	1.696	0.034
	Alginate-urea(1:2)	1.809	0.018
0.25	Alginate	3.609	0.055
	Alginate-urea(1:1)	8.222	0.028
	Alginate-urea(1:2)	—	—

EV: estimated variance.

Table 4. Modeling of uptake kinetics using the PSORE—Mono-component solutions (SD: 0.1 g (d.w.) l^{-1}).

C_0 (mmol Hg l^{-1})	Sorbent	$q_{e,exp.}$ (mmol g^{-1})	$q_{e,calc.}$ (mmol g^{-1})	$k_2 \times 10^2$ (g $mmol^{-1}$ min^{-1})	EV	R^2
0.05	Alginate	0.256	0.32	0.0191	6.51	0,9829
	Alginate-urea(1:1)	0.39	0.449	0.0198	6.08	0,9964
	Alginate-urea(1:2)	0.40	0.446	0.0250	4.71	0,9981
0.25	Alginate	0.460	0.58	0.0109	19.80	0,9859
	Alginate-urea(1:1)	1.003	1.04	0.0285	330.3	0,9991
	Alginate-urea(1:2)	—	—	—	—	

EV: estimated variance.

self-diffusivity of mercury in water (i.e., 5.08×10^{-8} m^2 min^{-1}); this confirms that the resistance to intraparticle diffusion is a controlling step in the global mass transfer. These values are consistent with the values obtained for Cd(II) and Cu(II) sorption using similar sorbents but higher than the values reported for Pb(II) [38].

The kinetic rates (k_2 for PSORE) are slightly higher for alginate derivative than for reference Alginate beads. This confirms the observation of kinetic profiles and the little increase in the time required for reaching equilibrium in the case of Alginate beads.

3.4. Sorption isotherms

Figure 7 shows the sorption isotherms obtained for the removal of Hg(II) from mono-component solutions at pH 3 using Alginate beads as the reference and urea-grafted materials (i.e., Alginate-urea(1:1) and Alginate-urea (1:2)). All the curves are characterized by a saturation plateau and a relative steep initial slope. The section 3 of Additional Material section reports some models commonly used for fitting sorption isotherms [65]. The Freundlich equation is characterized by a power-like shape (figure AM5(a), see Additional Material section) that is not consistent with the asymptotic trends of experimental curves.

The Freundlich isotherm computed data results with a lowest R^2 (0.89–0.94) value, the adsorption capacity value obtained for alginate and alginate-urea (1:1) is consistent with the other models and the experimental value. But the maximum adsorption capacity for the alginate-urea (1:2) (3.88 mmol g^{-1}), calculated on the basis of this model not agreed to experimental value (1.05 mmol g^{-1}), with a greater value of EV and with a lowest R^2 (0.89). According to the Freundlich model, the equilibrium is not reached (figure AM5(a), see Additional Material section).

The N value greater than 1 shows surface heterogeneity. This higher value revealed the heterogeneous nature of the adsorbent surface. This model determined that the Hg(II) adsorption is favorable and for this sorbent 'alginate-urea (1:2)' probably predicted an infinite monolayer coverage, this strong heterogeneous character for the second derivatives of alginate 'alginate-urea (1:2)' is confirmed by the value of 1/n or N, knowing that, when the 1/n value greater than 0 and less than 1 shows surface heterogeneity. The greater the 1/n value more will be the heterogeneity of the adsorbent surface [83].

On the contrary, the Langmuir sorption isotherm implicitly assumes an asymptotic shape: this equation fits relatively well with experimental data as seen in figure 7(a). Frequently this equation shows some weakness while fitting the curve in the concentration range corresponding to the highest curvature (here in around C_{eq}: 0.1 mmol Hg l^{-1}). Another model was applied using the combination of Langmuir and Freundlich concepts: the Sips equation generally allows getting a better statistical approximation because a new parameter is introduced in the equation; however, the model loses its physical significance compared to the mechanistic Langmuir equation. In addition, the Temkin model was also tested for evaluating the energy parameters associated to the sorption process (figure AM5(b), see Additional Material section). Table 5 reports the parameters of the different models and their respective correlation coefficients. As expected the Sips equation shows the better correlation coefficients for the three sorbents in agreement with figure 7(b). However, the correlation coefficients for the

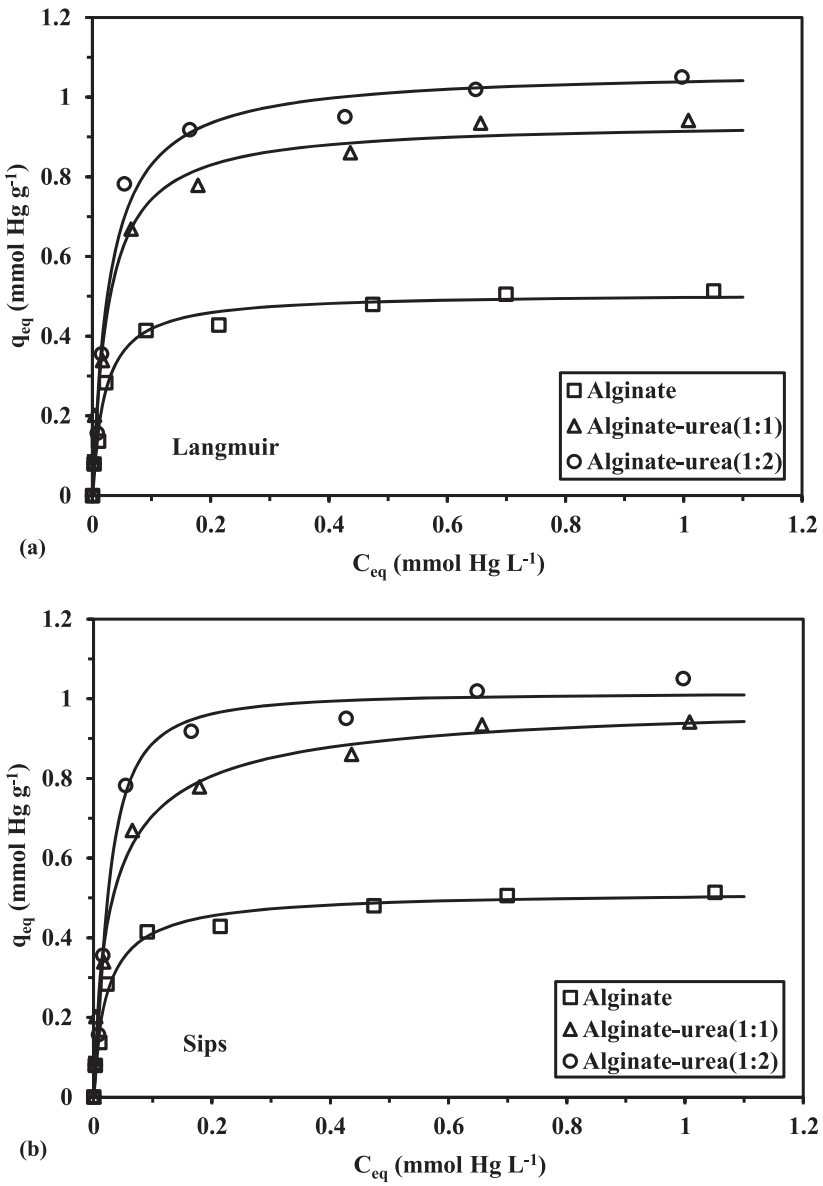

Figure 7. Hg(II) sorption isotherms using Alginate, Alginate-urea(1:1) and Alginate-urea(1:2), with modeling of experimental data with the Langmuir (a) and Sips (b) equations and the parameters reported in table 5 (contact time; t=300 min, dosage; SD = 0.1 $g.l^{-1}$, rotation speed (horizontal shaker) 150 rpm at a temperature T = 20 ± 1 °C, pH_i = 5.5).

Langmuir equation are relatively close to the values obtained for the sips model. Since the calculated sorption capacities at saturation of the monolayer $q_{m,L}$ for this model are very close to the experimental maximum sorption capacities ($q_{m,exp}$) the Langmuir equation will be preferred.

The grafting of urea almost doubles the maximum sorption capacity of Alginate beads, from 0.51 mmol Hg g^{-1} to 0.94 and 1.06 mmol Hg g^{-1}, for Alginate-urea(1:1) and Alginate-urea(1:2), respectively. Increasing the amount of urea grafted on the alginate backbone above a 1:1 molar ratio does not significantly improve sorption capacity. The affinity coefficient (i.e., b_L) slightly decreases with urea substitution: from 47.4 l $mmol^{-1}$ for Alginate beads to 38.2 and 35.0 l $mmol^{-1}$ for chemically-modified alginate. The heat of sorption deduced from Temkin modeling (i.e., b_T) is halved from 31.7 kJ mol^{-1} for Alginate beads to 16.9 and 13.7 kJ mol^{-1} for urea derivatives of alginate: this energetic criterion is consistent with the improvement of sorption efficiency with urea grafting on alginate backbone. The improvement in sorption capacity with urea grafting is obviously due to the increase in the density of sorption sites, but also to the specific affinity of relevant reactive groups. Indeed, N-based ligands (introduced by urea) are softer than O-based ligands (carboxylic groups of alginate) and they have a higher affinity for Hg(II) ions, which are considered soft acids according to the Pearson's rules (Hard & Soft Acids & Bases theory) [84]. The softness parameter for Hg(II) is close to +1.28 [85].

Tables 6 and 7 reports the Hg(II) sorption properties of a series of biopolymer-based sorbents. The variation in selected experimental conditions may strongly affect sorption properties and make difficult the comparison of

Table 5. Sorption isotherms—Parameters of the Langmuir, Freundlich, Sips and Temkin models.

Model	Parameter	Alginate	Alginate-urea (1:1)	Alginate-urea (1:2)
Experimental	$q_{m,exp}$	0.513	0.941	1.050
Langmuir	$q_{m,L}$	0.507	0.938	1.068
	b_L	47.4	38.2	35.0
	EV × 10^3	0.56	2.11	2.77
	R^2	0.983	0.990	0.990
Freundlich	k_F	0.555	1.035	3.88
	N	4.58	4.04	1.165
	EV × 10^3	3.74	10.9	27.9
	R^2	0.925	0.944	0.893
Sips	$q_{m,L}$	0.518	1.005	1.015
	b_S	30.79	14.01	163.8
	n_S	1.106	1.296	0.731
	EV × 10^3	0.63	1.37	1.44
	R^2	0.984	0.994	0.995
Temkin	A_T	1137.0	955.0	573.76
	b_T	31718.3	16911	13698
	EV × 10^3	1.40	2.37	10.7
	R^2	0.972	0.988	0.958

Table 6. Hg(II) sorption properties of selected biopolymers.

Material	pH	T (°C)	Equilibrium time (min)	Langmuir parameters		Reference
				$q_{m,L}$[a]	b_L[b]	
Alginate beads	3.3	25	—	1.40	123.0	[18]
PGA beads[c]	3.3	25	—	1.50	99.9	[18]
Pectin beads[d]	3.3	25	—	1.69	29.9	[18]
Alginate beads	5	25	60	0.16	13.2	[79]
AGCC[e] (5:2)	5	25	60	1.50	20.1	[79]
AGCC[e] (5:10)	5	25	60	3.32	25.3	[79]
Alginate beads	6	20	—	0.17	—	[86]
Alginate beads/live *F. trogii*	6	20	—	1.87	3.01	[86]
Alginate beads/inactivated *F. trogii*	6	20	—	2.12	8.22	[86]
Thiol-grafted chitosan beads	—	—	1200	7.98	—	[25]
Ca-alginate	—	—	—	0.16	—	[87]
Ca-alginate	5–6	25	—	0.19	—	[88]
Chitosan	6	25	—	3.74	—	[51]
Chitosan	—	—	—	4.01	—	[52]
GLA-crosslinked chitosan	6	25	—	0.38	—	[21]
Raw chitosan spheres	6	—	—	0.067	—	[23]
Raw chitosan membrane	6	—	—	0.13	—	[23]
GLA-crosslinked chitosan spheres	6	—	—	0.16	—	[23]
Chitosan bead thiol-grafted	—	—	—	1.47	—	[24]
Polyethyleneimine functionalized chitosan-lignin composite sponge	5.5	30	360	3.31	—	[40]
Magnetic thiol-modified chitosan beads	5	28	_	3.12	1.605	[89]
Alginate beads	5.5	20	300	0.51	46.7	*This work*
Alginate-urea(1:1) beads	5.5	20	300	0.94	80.2	*This work*
Alginate-urea(1:2) beads	5.5	20	300	1.07	74.6	*This work*

[a] mmol Hg g^{-1}.
[b] L $mmol^{-1}$.
[c] Alginate-polygalacturonate salts.
[d] Alginate-pectate beads.
[e] Calcium alginate beads containing different amount of cross-linked chitosan powder.

Table 7. Some others recent studies for mercury removal.

Material	pH	T(°C)	t/rotation speed	q_m mmol g^{-1}	Model	Reference
Cellulose−Lysine-Based Schiff Bases	5.0	50	60 min	1.29	Langmuir	[90]
A new functionalized hybrid adsorbent thiosemicarbazide grafting silica surface	7.0	25	30 min	0.05	Freundlich	[91]
Sulfur rich microporous polymer (SMP)	1.0	25	12 h	2.97	Langmuir	[92]
New spherical nanocellulose and thiol-based (SNC-3-MPA)	5.6	25	20 min	0.49	—	[93]
Magnetic spinel Fe_2CuO_4/rGO nanocomposite	7.0	24	60 min	6.23	Langmuir	[94]
Fe_3O_4-nanocellulose	7.0	At room T.	1000 rpm/90 min	4.62	Radke–Prausnitz	[95]
Aminophosphonic acid functionalized fiber ($PAN_{AP}F$)	6.0	At room T.	2 h	1.785	Langmuir	[96]
Chitosan- magnetic graphene oxide (OFMGO)	6.0	—	24 h	1.98	—	[97]
Chitosan-magnetic- magnetic graphene oxide (OFMGO)	7.0	—	5 h	1.80	—	[98]
L-cysteine doped polypyrrole (PPy@L-Cyst)	5.5	25	24 h	10.18	Langmuir	[99]
FeS nanoparticles	7.0	30	24 h	4.94	Langmuir	[100]
sodium carboxymethyl cellulose-FeS (CMC-FeS)				8.60		
gelatin-FeS and starch-FeS				9.66 and 9.9		
Melanin nanopigment obtained from marine source: *Pseudomonas stutzeri*	5.6	45	200 rpm	0.41	Langmuir	[101]
Guanyl-modified cellulose (Gu-MC)	6.0	25	3 h	0.24	Langmuir	[102]
Bentonite-alginate composite	6.0	30, 40 and 50	6 h/200 rpm	0.424, 0.555 and 0.618	Langmuir	[103]
Magnetic carbon nanotubes composite MWCNTs-Fe_3O_4	natural pH	25	2 h	1.19	Langmuir	[104]
Chitosan-Alginate Nanoparticles (CANPs)	5.0	30	90 min	1.08	Langmuir	[105]
polypyrrole/SBA-15 nanocomposite	8.0	At room T.	60 min	0.997	Langmuir	[106]
Thiourea Functionalized polypropylene fiber grafted acrylic acid	5.0	25	2 h/150 rpm	0.26	Langmuir	[107]
Polyamide magnetic palygorskite (MPG) by polyamide	5.0	—	30 min/120 rpm	1.06	Langmuir	[108]
L-Cysteine functionalized bagasse cellulose nanofibers	6.8	30	30 min	0.58	Langmuir	[109]
hydrazide-micromagnetite chitosan derivative	5.0	22	48 h	1.82	Langmuir	[110]
amide functionalized cellulose from sugarcane bagasse	4.5	30	24 h/120 rpm	1.124	Langmuir	[111]

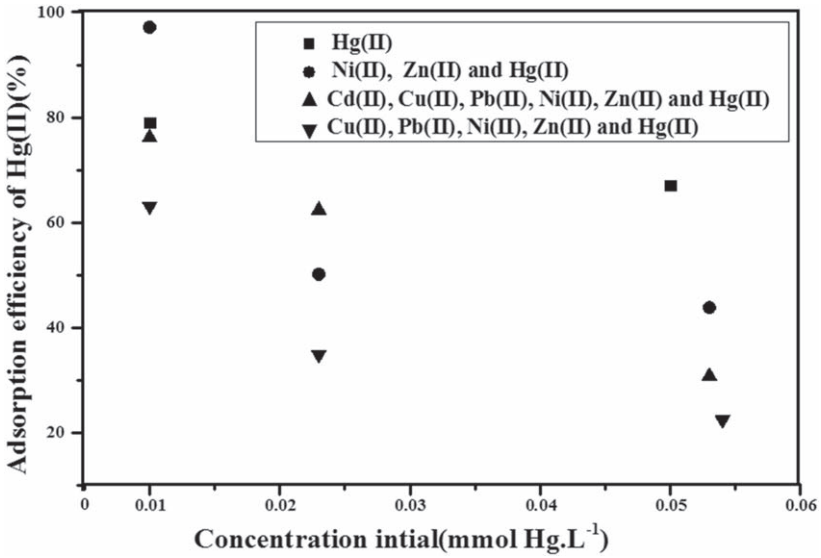

Figure 8. Influence of other co-existing metal ions on Hg(II) adsorption by Alginate-urea (1:1) synthesized under the same conditions at pH = 5.5 and at a room temperature.

performances. The sorption properties of urea-derivatives of alginate are comparable to most of the biopolymer-based sorbents; however, the capacities are several times higher for biopolymers grafted with sulfur derivatives (thiol, thiourea, etc). The very favorable behavior of sulfur-based derivatives is directly explained by the much softer behavior of S-based ligands (compared to N-based and even more O-based ligands). It is noteworthy that synthetic resins may exhibit higher sorption capacities such as magnetic glycidyl methacrylate resin (2.8 mmol Hg g^{-1}), crosslinked quaternary amide-sulfonamide resin (3 mmol Hg g^{-1}); though synthetic resins (such as resin-bound 2-pyridinethiol) have been also used with significantly lower capacities (0.28 mmol Hg g^{-1}).

4. Effect of coexisting metal ions—competitive adsorption study

The difficulty in removal of heavy metals at low concentrations (2, 5 and 10 mg l^{-1}) has led to the exploration of efficient adsorbents for removal of these metals, especially mercury due to its toxicity and strict standards (table 1) related to its presence in drinking water (0.5–2 μg l^{-1}) [46] and industrial effluents (0.01 mg l^{-1}).

In order to testing the effect of competition of other metal ions in the efficiency of mercury removal, we have prepared five solutions with different metals compositions and different concentrations. The mass of 0.05 g of alginate modified were added, separately at 500 ml of solution, at the initial pH of the solution 5.5 and temperature of 20 °C.

In this study, we have increased the concentration of mercury in multicomponent solutions (0.01, 0.02 and 0.05 mmol Hg/L), in order to compare the results with mercury adsorption in monometallic solution.

The sorption isotherms on mono-component solutions have shown a better potential of the sorbents for mercury at low concentrations, this is confirmed by a study of the selectivity and efficacies of this treatment by bi-components, three- and multi-components metal solutions in the same conditions. The selectivity for mercury in multi-components solutions is influenced by the initial concentration of the solution as well as the nature of the elements coexisting in solution. It can be seen that the efficiency decreases from 97.47 to 8.7% according to the operating conditions (figure 8 and table 8).

The result of study of the sorption of various examples of metallic solutions at 4 mg metal l^{-1} is shown in figure 9. It should be noted that in the binary Pb(II)/Hg(II) solution and multiple Cd(II), Cu(II), Pb(II) and Hg(II) solutions, the adsorbent proclaims a high affinity for lead relative to mercury (see figure 9). It is obvious that the alginate-urea (1:1) shows good adsorption for Pb(II) with an adsorption capacity of 47–49 mg g^{-1} and an efficiency ranged between 97.45%–99.58% (see figure 9). This is reasonable due to that new functional groups has a strong affinity for this metal, similarly the Cu(II) give a good affinity compared with other metals. The capacity adsorption of Cd(II), Zn(II) and Ni(II) is low compared to Cu(II) and Pb(II).

For the Mercury, efficiency changes also depending on the composition of the solution. when mercury is found alone in solution, efficiency is 84.9% (40.5 mg g^{-1}), then varies to 52.35, 8.7, 54.24, 62.36 and 34.80%

Table 8. Influence of other co-existing metal ions on Hg(II) adsorption at pH = 5.5 and T = 20 °C.

Elements in the solution of metals (+Hg(II))	Hg(II)	Pb(II)+Hg(II)	Cd(II), Cu(II), Hg(II) and Pb(II)	Zn(II) Ni(II) and Hg(II)	Cd(II), Cu(II), Pb(II), Zn(II), Hg(II) and Ni(II)	Cu(II), Pb(II), Zn(II), Hg(II) and Ni(II)
Concentration (mg metal l^{-1})				Hg(II) adsorption efficiency(%)		
2	81.01	59.91	20.18	97.47	76.17	64.89
4	84.91	52.35	8.7	54.24	62.36	34.80
10	67.00	50.84	12.88	43.30	30.73	22.41

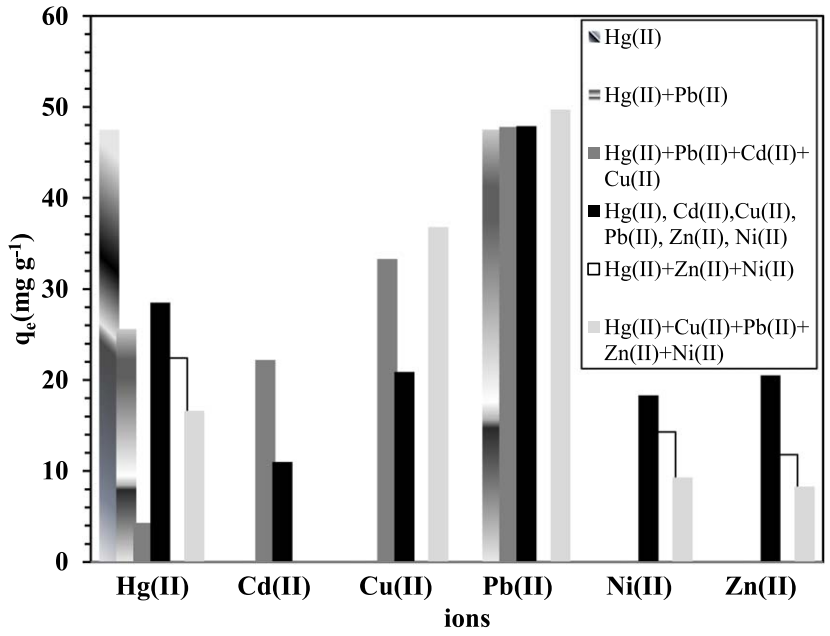

Figure 9. Adsorption capacities of alginate-urea (1:1) for various example of metal solutions (C_0 = 4 mg metal l^{-1}) with different components.

with the variation of the solution composition, corresponding to the five examples of solutions presented in figure 9. However, in any case, modified adsorbents ' alginate-urea (1:1) and alginate-urea (1:2)' have shown a better efficiency for the treatment of complex solutions.

5. Mechanism of adsorption

The adsorption mechanism was investigated by the discussions of the results obtained in the adsorption kinetics, isotherms and ESEM-EDX analysis, similarly to the study presented recently by [96].

Various kinetics and isotherm models were used to evaluate the adsorption data. The results obtained by the PSORE model suggests that the adsorption process is a chemical interaction between metal ions and active sites rather than a simple physical adsorption process [112]. The modeling of the results obtained for alginate-urea (1:1) and alginate-urea (1:2) with PSORE model and PFORE (C_0 = 0.05 mmol l^{-1}) gives high values of R^2 almost equal (see tables 4 and AM1, see Additional Material section).

In addition, the adsorption data of Hg(II) on the three adsorbents, fit with the Langmuir model implies that the adsorption process could be considered as monolayer adsorption and all the active sites on the adsorbent are energetically identical [113].

The possible interaction of Hg(II) with alginate-urea is shown in figure 10. This figure gives the possible form of alginate-urea and the proposed mechanism of their sorption. In the selected pH, the protonation of amine groups decreases progressively, therefore, the Hg(II) ions are bound with the nitrogen atoms of the amine groups through coordination. Moreover, the negatively charged of carboxylic group hold the positively charged Hg(II) ions though electrostatic forces. *F.C. Wu et al* show that the carboxyl and unprotonated amino groups can serve as coordination and electrostatic interaction sites for the sorption of transition metals [114].

The results obtained in this study can be elucidated with HSAB concept. Therefore, Hg^{2+} ions are soft acids and the modified adsorbent, having amine groups (-NH_2), are classified as hard base; so they provide a strong interaction in Hg^{2+} metallic solution. On the basis of this theory, O-ligands (carboxylic acid groups) have more affinity for hard acids than N-ligands (amine groups) and soft acids have more affinity for -N ligands (amine groups) than -O ligands (carboxylic groups) [38]. This confirms the coordination interactions between R-NH_2 and Hg^{2+}. According S. Huang *et al* (2016) the reason of these preference is that soft acid of Hg(II) ion offers high affinity toward soft bases of –C = O and C–CO–C groups and middle-soft bases of –NH–, –N = , and –NH_2 groups [50]. However, when borderline acidic metal ions, such as Pb(II) or Cu(II) are present in metallic solution, they can react with the two groups –O and –N and lose their selective nature when competitive ions are present.

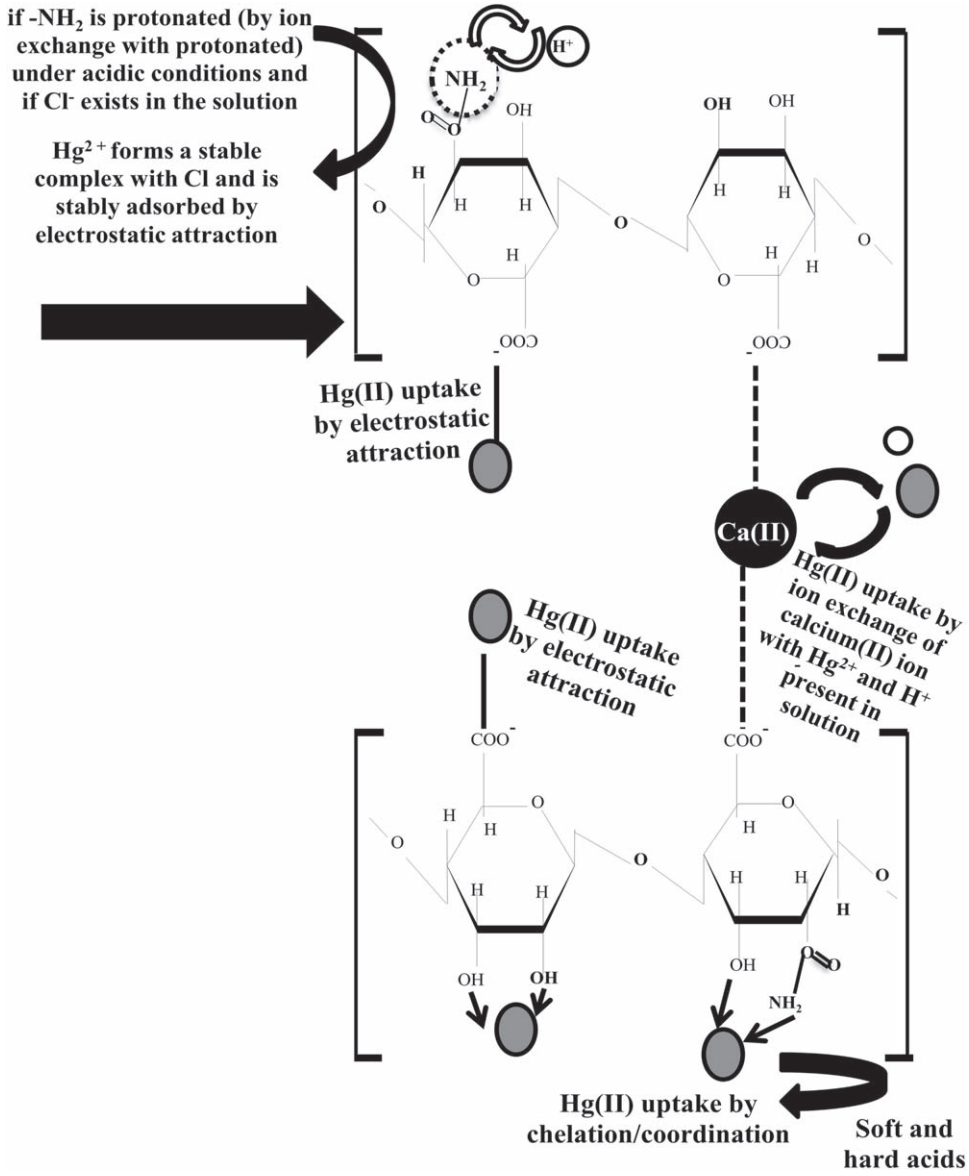

Figure 10. Proposed mechanism of Hg(II) adsorption.

6. Conclusion

This study demonstrated the feasibility of removing mercury from aqueous solutions using alginate-urea compared to alginate who has a low affinity towards this metal, the addition of the amine function in the structure of the alginate improve the efficiency of mercury sorption, therefore we conclude that the amine is the effective function in the Mercury sorption, this is confirmed by the great affinity of chitosan towards this metal. In addition, the change in the quantity of urea to improve the efficiency this gives us an idea on the effect of the quantity grafting on the structure of the new material *(the increase in -NH_2 slightly increased the sorption efficiency and consequently we can still improve the capacity if we choose the right grafting parameters)*. According to the results obtained in this study, it is necessary to choose well the added function (–NH_2 or others function), the way and above all the cost because generally we want to modify the biosorbents to reduce the cost of the operation of biosorption to maintain or/and adapt the basic properties. So the researchers must compare the need for modification with respect to the basic materials, and for each modification we ask the question what are the contributions for each modification compared to the basic materials.

The results suggested that the grafting of urea on Alginate beads allows increasing the sorption capacity of the biopolymer for Hg(II). At optimum adsorption conditions obtained in this study (pH = 5.5, SD = 0.1 g/l), alginate-urea give the adsorption yield were up to 80% at low concentrations in the range of 2 to 10 mg $Hg\,l^{-1}$. However, it was demonstrated that doubling the amount of urea introduced in the reactor for the synthesis of

urea derivatives of alginate is slightly significantly increase sorption performance (0.9 mmol g^{-1} for the alginate-urea (1:1) compared to 1.07 mmol g^{-1} for the alginate-urea(1:2)): this amount of 1.116 g of urea for 3 g of alginate can be changed for the augmentation of the percent of amino groups in the alginate-urea.

The increase in the density of the reactive groups and the higher affinity of N-based ligands (compared to O-based ligands of carboxylic groups) can both explain the enhancement of sorption properties for soft-acid Hg(II) ion.

Sorption properties are controlled by the pH: metal binding is increased with pH due to the deprotonation of reactive groups and sorption properties have been tested at pH 5.5. Sorption isotherms are finely fitted with the Langmuir and the Sips equations. Maximum sorption capacities reached 0.51, 0.94 and 1.07 mmol Hg g^{-1} for Alginate beads, Alginate-urea (1:1) and Alginate-urea (1:2) beads, respectively. Uptake kinetics are well described by the pseudo-second order rate equation and the resistance to intraparticle diffusion (RIDE, Crank-based equation). The intraparticle diffusion coefficient is about one order of magnitude lower than the self-diffusivity of Hg(II) in water.

Complementary experiments would be necessary to verify the selectivity of the sorbents for Hg(II) or at least the impact of other competitor ions (anions and cations) on metal binding, with other different concentration. In addition, it would be necessary checking the possibility to desorb the metals from loaded solid phases with the target of concentrating the hazardous contaminant but also verify the recyclability of the sorbent (to make the process competitive).

Acknowledgments

This research project was financially supported by Grant PNE (Programme National Exceptionnel, Ministère de l'Enseignement Supérieur et de la Recherche Scientifique—Algérie). The authors acknowledge the Jean-Claude Roux (Ecole des Mines d'Alès, C2MA) for his technical support for SEM and ESEM-EDX analyses.

Data availability statement

All data that support the findings of this study are included within the article (and any supplementary files).

ORCID iDs

Benettayeb A https://orcid.org/0000-0003-2647-1698

References

[1] Mancini M V, Spreti N, Di Profio P and Germani R 2013 Understanding mercury extraction mechanism in ionic liquids *Sep. Purif. Technol.* **116** 294–9
[2] Wu C Y, Chen S S, Zhang D Z and Kobayashi J 2017 Hg removal and the effects of coexisting metals in forward osmosis and membrane distillation *Water Sci. Technol.* **75** 2622–30
[3] Ozgur C, Coskun S, Akcil A, Beyhan M, Üncü I S and Civelekoglu G 2016 Combined oxidative leaching and electrowinning process for mercury recovery from spent fluorescent lamps *Waste Manag.* **57** 215–9
[4] Chatterjee M, Srivastava B, Barman M K and Mandal B 2016 Combined cation-exchange and solid phase extraction for the selective separation and preconcentration of zinc, copper, cadmium, mercury and cobalt among others using azo-dye functionalized resin *J. Chromatogr.* A **1440** 1–14
[5] Takagai Y, Shibata A, Kiyokawa S and Takase T 2011 Synthesis and evaluation of different thio-modified cellulose resins for the removal of mercury (II) ion from highly acidic aqueous solutions *J. Colloid Interface Sci.* **353** 593–7
[6] Tangestaninejad S, Mohammadpoor-Baltork I, Moghadam M, Mirkhani V, Iravani M R and Ahmadi V 2012 Readily prepared resin-bound 2-pyridinethiol and its application for removal of mercury ions *J. Iran. Chem. Soc.* **9** 61–5
[7] Yavuz E, Turan G T and Alkazan B F S S 2015 Preparation of crosslinked quaternary amide-sulfonamide resin for removal of mercury ions from aqueous solutions *Desalin. Water Treat.* **56** 2145–53
[8] Guibal E, Gavilan K C, Bunio P, Vincent T and Trochimczuk A 2008 CYPHOS IL 101 (tetradecyl(trihexyl)phosphonium chloride) immobilized in biopolymer capsules for Hg(II) recovery from HCl solutions *Sep. Sci. Technol.* **43** 2406–33
[9] Bao S, Li K, Ning P, Peng J, Jin X and Tang L 2017 Highly effective removal of mercury and lead ions from wastewater by mercaptoamine-functionalised silica-coated magnetic nano-adsorbents: behaviours and mechanisms *Appl. Surf. Sci.* **393** 457–66
[10] Barragán P P, Macedo M M G and Olguín M T 2017 Cadmium sorption by sodium and thiourea-modified zeolite-rich tuffs *J. Environ. Sci. (China)* **52** 39–48
[11] Johari K, Saman N and Mat H 2014 A comparative evaluation of mercury(II) adsorption equilibrium and kinetics onto silica gel and sulfur-functionalised silica gels adsorbents *Can. J. Chem. Eng.* **92** 1048–58
[12] Ravi S, Selvaraj M, Park H, Chun H-H and Ha C-S 2014 Novel hierarchically dispersed mesoporous silica spheres: effective adsorbents for mercury from wastewater and a thermodynamic study *New J. Chem.* **38** 3899
[13] Kadirvelu K, Kavipriya M, Karthika C, Vennilamani N and Pattabhi S 2004 Mercury (II) adsorption by activated carbon made from sago waste *Carbon N. Y.* **42** 745–52

[14] Namasivayam C and Kadirvelu K 1999 Uptake of mercury (II) from wastewater by activated carbon from an unwanted agricultural solid by-product: coirpith *Carbon N. Y.* **37** 79–84
[15] Ngah W S W and Hanafiah M A K M 2008 Biosorption of copper ions from dilute aqueous solutions on base treatedrubber (Hevea brasiliensis) leaves powder: kinetics, isotherm, and biosorption mechanisms *J. Environ. Sci.* **20** 1168–76
[16] Xu F, Zhu T T, Rao Q Q, Shui S W, Li W W, He H B and Yao R S 2017 Fabrication of mesoporous lignin-based biosorbent from rice straw and its application for heavy-metal-ion removal *J. Environ. Sci. (China)* **53** 132–40
[17] Wan Maznah W O, Al-Fawwaz A T and Surif M 2012 Biosorption of copper and zinc by immobilised and free algal biomass, and the effects of metal biosorption on the growth and cellular structure of Chlorella sp. and Chlamydomonas sp. isolated from rivers in Penang, Malaysia *J. Environ. Sci. (China)* **24** 1386–93
[18] Cataldo S, Gianguzza A, Pettignano A and Villaescusa I 2013 Mercury(II) removal from aqueous solution by sorption onto alginate, pectate and polygalacturonate calcium gel beads. A kinetic and speciation based equilibrium study *React. Funct. Polym.* **73** 207–17
[19] Allouche F N, Guibal E and Mameri N 2014 Preparation of a new chitosan-based material and its application for mercury sorption *Colloids Surfaces A Physicochem. Eng. Asp.* **446** 224–32
[20] Vieira R S and Beppu M M 2006 Interaction of natural and crosslinked chitosan membranes with Hg(II) ions *Colloids Surfaces A Physicochem. Eng. Asp.* **279** 196–207
[21] Vieira R S, Guibal E, Silva E A and Beppu M M 2007 Adsorption and desorption of binary mixtures of copper and mercury ions on natural and crosslinked chitosan membranes *Adsorption* **13** 603–11
[22] Cathell M D, Szewczyk J C and Schauer C L 2010 Organic modification of the polysaccharide alginate *Mini. Rev. Org. Chem.* **7** 61–7
[23] Jeon C and Höll W H 2003 Chemical modification of chitosan and equilibrium study for mercury ion removal *Water Res.* **37** 4770–80
[24] Jeon C and Kwang H P 2005 Adsorption and desorption characteristics of mercury(II) ions using aminated chitosan bead *Water Res.* **39** 3938–44
[25] Merrifield J D, Davids W G, MacRae J D and Amirbahman A 2004 Uptake of mercury by thiol-grafted chitosan gel beads *Water Res.* **38** 3132–8
[26] Carro L, Barriada J L, Herrero R and Sastre de Vicente M E 2011 Adsorptive behaviour of mercury on algal biomass: competition with divalent cations and organic compounds *J. Hazard. Mater.* **192** 284–91
[27] Shanab S, Essa A and Shalaby E 2012 Bioremoval capacity of three heavy metals by some microalgae species (Egyptian Isolates) *Plant Signal. Behav.* **7** 392–9
[28] Bayramoğlu G, Tuzun I, Celik G, Yilmaz M and Arica M Y 2006 Biosorption of mercury(II), cadmium(II) and lead(II) ions from aqueous system by microalgae Chlamydomonas reinhardtii immobilized in alginate beads *Int. J. Miner. Process.* **81** 35–43
[29] Khotimchenko M, Kovalev V and Khotimchenko Y 2008 Comparative equilibrium studies of sorption of Pb(II) ions by sodium and calcium alginate *J. Environ. Sci.* **20** 827–31
[30] Rahman A H A, Teo C L, Idris A, Misran E and Leong S A N 2015 Polyvinyl alcohol-alginate ferrophoto gels for mercury(II) removal *J. Ind. Eng. Chem.* **33** 190–6
[31] Sinha A, Pant K K and Khare S K 2012 Studies on mercury bioremediation by alginate immobilized mercury tolerant *Bacillus cereus* cells *Int. Biodeterior. Biodegrad.* **71** 1–8
[32] Son B C, Park K, Song S H and Yoo Y J 2004 Selective biosorption of mixed heavy metal ions using polysaccharides *Korean J. Chem. Eng.* **21** 1168–72
[33] Davis T A, Volesky B and Mucci A 2003 A review of the biochemistry of heavy metal biosorption by brown algae *Water Res.* **37** 4311–30
[34] Qiu Y-W 2015 Bioaccumulation of heavy metals both in wild and mariculture food chains in Daya Bay, South China *Estuar. Coast. Shelf Sci.* **163** 7–14
[35] Jang L K, Lopez S L, Eastman S L and Pryfogle P 1991 Recovery of copper and cobalt by biopolymer gels *Biotechnol. Bioeng.* **37** 266–73
[36] Tang Z, Peng S, Hu S and Hong S 2017 Enhanced removal of bisphenol-AF by activated carbon-alginate beads with cetyltrimethyl ammonium bromide *J. Colloid Interface Sci.* **495** 191–9
[37] Cataldo S, Gianguzza A, Merli M, Muratore N, Piazzese D and Turco Liveri M L 2014 Experimental and robust modeling approach for lead(II) uptake by alginate gel beads: Influence of the ionic strength and medium composition *J. Colloid Interface Sci.* **434** 77–88
[38] Benettayeb A, Guibal E, Morsli A and Kessas R 2017 Chemical modification of alginate for enhanced sorption of Cd(II), Cu(II) and Pb(II) *Chem. Eng. J.* **316** 704–14
[39] Benettayeb A, Guibal E, Bhatnagar A, Morsli A and Kessas R 2021 Effective removal of nickel (II) and zinc (II) in mono-compound and binary systems from aqueous solutions by application of alginate-based materials *Int. J. Environ. Anal. Chem.* **0** 1–22
[40] Zhang D, Wang L, Zeng H, Rhimi B and Wang C 2020 Novel polyethyleneimine functionalized chitosan-lignin composite sponge with nanowall-network structures for fast and efficient removal of Hg(ii) ions from aqueous solution *Environ. Sci. Nano* **7** 793–802
[41] Naushad M, Vasudevan S, Sharma G, Kumar A and Alothman Z A 2016 Adsorption kinetics, isotherms, and thermodynamic studies for Hg^{2+} adsorption from aqueous medium using alizarin red-S-loaded amberlite IRA-400 resin *Desalin. Water Treat.* **57** 18551–9
[42] Machell J, Prior K, Allan R and Andresen J M 2015 The water energy food nexus—challenges and emerging solutions *Environ. Sci. Water Res. Technol.* **1** 15–6
[43] Vianna A, dos S, de Matos E P, de Jesus I M, Asmus C I R F and Câmara V de M 2019 Human exposure to mercury and its hematological effects: a systematic revie *Cad. Saude Publica* **35** 1–22
[44] Hong Y S, Kim Y M and Lee K E 2012 Methylmercury exposure and health effects *J. Prev. Med. Public Heal.* **45** 353–63
[45] Brião G de V, de Andrade J R, da Silva M G C and Vieira M G A 2020 Removal of toxic metals from water using chitosan-based magnetic adsorbents. A review *Environ. Chem. Lett.* **18** 1145–68
[46] Xu J, Cao Z, Zhang Y, Yuan Z, Lou Z, Xu X and Wang X 2018 A review of functionalized carbon nanotubes and graphene for heavy metal adsorption from water: preparation, application, and mechanism *Chemosphere* **195** 351–64
[47] Plaza J, Viera M, Donati E and Guibal E 2011 Biosorption of mercury by Macrocystis pyrifera and Undaria pinnatifida: influence of zinc, cadmium and nickel *J. Environ. Sci.* **23** 1778–86
[48] Çelik Z, Gülfen M and Aydin A O 2010 Synthesis of a novel dithiooxamide-formaldehyde resin and its application to the adsorption and separation of silver ions *J. Hazard. Mater.* **174** 556–62
[49] Liu Y, Zhang W, Zhao C, Wang H, Chen J, Yang L, Feng J and Yan W 2019 Study on the synthesis of poly(pyrrole methane)s with the hydroxyl in different substituent position and their selective adsorption for Pb^{2+} *Chem. Eng. J.* **361** 528–37
[50] Huang S, Ma C, Liao Y, Min C, Du P and Jiang Y 2016 Removal of mercury(II) from aqueous solutions by adsorption on Poly(1-amino-5-chloroanthraquinone) nanofibrils: equilibrium, kinetics, and mechanism studies *J. Nanomater.* **2016** 1–11
[51] Shafaei A, Ashtiani F Z and Kaghazchi T 2007 Equilibrium studies of the sorption of Hg(II) ions onto chitosan *Chem. Eng. J.* **133** 311–6
[52] Bailey S E, Olin T J, Bricka R M and Adrian D D 1999 A review of potentially low-cost sorbents for heavy metals *Water Res.* **33** 2469–79

[53] Adewuyi A 2020 Chemically modified biosorbents and their role in the removal of emerging pharmaceutical waste in the water system *Water* **12** 1551
[54] Agulhon P, Robitzer M, David L and Quignard F 2012 Structural regime identification in ionotropic alginate gels: influence of the cation nature and alginate structure *Biomacromolecules* **13** 215–20
[55] Atia A A, Donia A M and Elwakeel K Z 2005 Adsorption behaviour of non-transition metal ions on a synthetic chelating resin bearing iminoacetate functions *Sep. Purif. Technol.* **43** 43–8
[56] Donia A M, Atia A A and Abouzayed F I 2012 Preparation and characterization of nano-magnetic cellulose with fast kinetic properties towards the adsorption of some metal ions *Chem. Eng. J.* **191** 22–30
[57] Elwakeel K Z, Atia A A and Guibal E 2014 Fast removal of uranium from aqueous solutions using tetraethylenepentamine modified magnetic chitosan resin *Bioresour. Technol.* **160** 107–14
[58] Lopez-Ramon M V, Stoeckli F, Moreno-Castilla C and Carrasco-Marin F 1999 On the characterization of acidic and basic surface sites on carbons by various techniques *Carbon N. Y.* **37** 1215–21
[59] Do D D 1998 *Adsorption Analysis: Equilibrium and Kinetics* (https://doi.org/10.1142/p111)
[60] Lagergren S 1898 About the theory of so-called adsorption of soluble substances *Kungliga Svenska Vetenskapsakademiens* **24** 1–39
[61] Ho Y S and McKay G 1999 Pseudo-second order model for sorption processes *Process Biochem.* **34** 451–65
[62] Mohan D, Gupta V K, Srivastava S K and Chander S 2001 Kinetics of mercury adsorption from wastewater using activated carbon derived from fertilizer waste *Colloids Surf.,* A **177** 169–81
[63] Tien C 1994 *Adsorption Calculations and Modeling* (Newton, MA: Butterworth-Heinemann)
[64] Crank J 1975 *The Mathematics of Diffusion* 2nd edn (Oxford, U.K: Oxford University Press)
[65] Hameed B H and Foo K Y 2010 Insights into the modeling of adsorption isotherm systems *Chem. Eng. J.* **156** 2–10
[66] Langmuir I 1918 The adsorption of gases on plane surfaces of glass, mica and platinum *J. Am. Chem. Soc.* **40** 1361–403
[67] Hameed B H, Tan I A W and Ahmad A L 2008 Adsorption isotherm, kinetic modeling and mechanism of 2,4,6-trichlorophenol on coconut husk-based activated carbon *Chem. Eng. J.* **144** 235–44
[68] Khan A, Badshah S and Airoldi C 2011 Biosorption of some toxic metal ions by chitosan modified with glycidylmethacrylate and diethylenetriamine *Chem. Eng. J.* **171** 159–66
[69] Mohan D, Kumar H, Sarswat A, Alexandre-Franco M and Pittman C U 2014 Cadmium and lead remediation using magnetic oak wood and oak bark fast pyrolysis bio-chars *Chem. Eng. J.* **236** 513–28
[70] Rocha L S, Almeida Â, Nunes C, Henriques B, Coimbra M A, Lopes C B, Silva C M, Duarte A C and Pereira E 2016 Simple and effective chitosan based films for the removal of Hg from waters: equilibrium, kinetic and ionic competition *Chem. Eng. J.* **300** 217–29
[71] Temkin P V 1940 Kinetics of ammonia synthesis on promoted iron catalysts *Acta Physiochim.* **12** 217–22
[72] Haug A 1961 Dissociation of alginic acid *Acta Chem. Scand.* **15** 950–15952
[73] Guzmán J, Saucedo I, Navarro R, Revilla J and Guibal E 2002 Vanadium interactions with chitosan: influence of polymer protonation and metal speciation *Langmuir* **18** 1567–73
[74] Guzman J, Saucedo I, Revilla J, Navarro R and Guibal E 2003 Copper sorption by chitosan in the presence of citrate ions: Influence of metal speciation on sorption mechanism and uptake capacities *Int. J. Biol. Macromol.* **33** 57–65
[75] Gustafsson 2013 Visual MINTEQ, ver. 3.1, ver. 3.1 ed. KTH, Royal Institute of Technology, (url: https://vminteq.lwr.kth.se/; accessed May 2017) Stockholm, Sweden. J P
[76] Dunham-Cheatham S, Farrell B, Mishra B, Myneni S and Fein J B 2014 The effect of chloride on the adsorption of Hg onto three bacterial species *Chem. Geol.* **373** 106–14
[77] Arias Arias F E, Beneduci A, Chidichimo F, Furia E and Straface S 2017 Study of the adsorption of mercury (II) on lignocellulosic materials under static and dynamic conditions *Chemosphere* **180** 11–23
[78] Bulbul Sonmez H, Senkal B F, Sherrington D C and Bicak N 2003 Atom transfer radical graft polymerization of acrylamide from N-chlorosulfonamidated polystyrene resin, and use of the resin in selective mercury removal *React. Funct. Polym.* **55** 1–8
[79] Chang Y H, Huang C F, Hsu W J and Chang F C 2007 Removal of Hg^{2+} from aqueous solution using alginate gel containing chitosan *J. Appl. Polym. Sci.* **104** 2896–905
[80] Chen D, Lewandoswki Z, Roe F and Surapaneni P 1993 Diffusivity of Cu^{2+} in calcium alginate gel beads *Biotechnol. Bioeng.* **41** 755–60
[81] Ruiz M, Sastre A and Guibal E 2002 Pd and Pt recovery using chitosan gel beads. I. Influence of the drying process on diffusion properties *Sep. Sci. Technol.* **37** 2143–66
[82] Lagoa R and Rodrigues J R 2009 Kinetic analysis of metal uptake by dry and gel alginate particles *Biochem. Eng. J.* **46** 320–6
[83] Jurinak J J, Baes C F and Mesmer R 1976 *The Hydrolysis of Cations* **40** 245–6
[84] Persson I 2010 Hydrated metal ions in aqueous solution: how regular are their structures? *Pure Appl. Chem.* **82** 1901–17
[85] Marcus Y 1997 *Ion Properties* (New York: Marcel Dekker, Inc)
[86] Arica M Y, Bayramoğlu G, Yilmaz M, Bektaş S and Genç Ö 2004 Biosorption of Hg^{2+}, Cd^{2+}, and Zn^{2+} by Ca-alginate and immobilized wood-rotting fungus Funalia trogii *J. Hazard. Mater.* **109** 191–9
[87] Kaçar Y, Arpa Ç, Tan S, Denizli A, Genç Ö and Arica M Y 2002 Biosorption of Hg(II) and Cd(II) from aqueous solutions: comparison of biosorptive capacity of alginate and immobilized live and heat inactivated Phanerochaete chrysosporium *Process Biochem.* **37** 601–10
[88] Elwakeel K Z and Guibal E 2016 Potential use of magnetic glycidyl methacrylate resin as a mercury sorbent: from basic study to the application to wastewater treatment *J. Environ. Chem. Eng.* **4** 3632–45
[89] Zhou L, Wang Y, Liu Z and Huang Q 2009 Characteristics of equilibrium, kinetics studies for adsorption of Hg(II), Cu(II), and Ni(II) ions by thiourea-modified magnetic chitosan microspheres *J. Hazard. Mater.* **161** 995–1002
[90] Kumari S and Chauhan G S 2014 New cellulose—lysine schiff -base-based sensor—adsorbent for mercury ions *ACS Appl. Mater. Interfaces* **6** 5908–17
[91] Ali Z, Ahmad R, Khan A and Adalata B 2018 Complexation of Hg(II) ions with a functionalized adsorbent: a thermodynamic and kinetic approach *Prog. Nucl. Energy* **105** 146–52
[92] Xu D, Wu W D, Qi H J, Yang R X and Deng W Q 2018 Sulfur rich microporous polymer enables rapid and efficient removal of mercury(II) from water *Chemosphere* **196** 174–81
[93] Ram B and Chauhan G S 2018 New spherical nanocellulose and thiol-based adsorbent for rapid and selective removal of mercuric ions *Chem. Eng. J.* **331** 587–96
[94] Zandi-Atashbar N, Ensafi A A and Ahoor A H 2018 Magnetic Fe_2CuO_4/rGO nanocomposite as an efficient recyclable catalyst to convert discard tire into diesel fuel and as an effective mercury adsorbent from wastewater *J. Clean. Prod.* **172** 68–80
[95] Zarei S, Niad M and Raanaei H 2018 The removal of mercury ion pollution by using Fe_3O_4-nanocellulose: synthesis, characterizations and DFT studies *J. Hazard. Mater.* **344** 258–73

[96] Xu G, Wang L, Xie Y, Tao M and Zhang W 2018 Highly selective and efficient adsorption of Hg^{2+} by a recyclable aminophosphonic acid functionalized polyacrylonitrile fiber *J. Hazard. Mater.* **344** 679–88
[97] Kyzas G Z, Travlou N A and Deliyanni E A 2014 The role of chitosan as nanofiller of graphite oxide for the removal of toxic mercury ions *Colloids Surfaces B Biointerfaces* **113** 467–76
[98] Zhang Y, Yan T, Yan L, Guo X, Cui L, Wei Q and Du B 2014 Preparation of novel cobalt ferrite/chitosan grafted with graphene composite as effective adsorbents for mercury ions *J. Mol. Liq.* **198** 381–7
[99] Ballav N, Das R, Giri S, Muliwa A M, Pillay K and Maity A 2018 l-cysteine doped polypyrrole (PPy@L-Cyst): a super adsorbent for the rapid removal of Hg+2 and efficient catalytic activity of the spent adsorbent for reuse *Chem. Eng. J.* **345** 621–30
[100] Sun Y, Liu Y, Lou Z, Yang K, Lv D, Zhou J, Baig S A and Xu X 2018 Enhanced performance for Hg(II) removal using biomaterial (CMC/gelatin/starch) stabilized FeS nanoparticles: stabilization effects and removal mechanism *Chem. Eng. J.* **344** 616–24
[101] Manirethan V, Raval K, Rajan R, Thaira H and Balakrishnan R M 2018 Kinetic and thermodynamic studies on the adsorption of heavy metals from aqueous solution by melanin nanopigment obtained from marine source: Pseudomonas stutzeri *J. Environ. Manage.* **214** 315–24
[102] Kenawy I M, Hafez M A H, Ismail M A and Hashem M A 2018 Adsorption of Cu(II), Cd(II), Hg(II), Pb(II) and Zn(II) from aqueous single metal solutions by guanyl-modified cellulose *Int. J. Biol. Macromol.* **107** 1538–49
[103] Sellaoui L, Soetaredjo F E, Ismadji S, Benguerba Y, Dotto G L, Bonilla-Petriciolet A, Rodrigues A E, Ben L A and Erto A 2018 Equilibrium study of single and binary adsorption of lead and mercury on bentonite-alginate composite: experiments and application of two theoretical approaches *J. Mol. Liq.* **253** 160–8
[104] Sadegh H, Ali G A M, Makhlouf A S H, Chong K F, Alharbi N S, Agarwal S and Gupta V K 2018 MWCNTs-Fe_3O_4 nanocomposite for Hg(II) high adsorption efficiency *J. Mol. Liq.* **258** 345–53
[105] Dubey R, Bajpai J and Bajpai A K 2016 Chitosan-alginate nanoparticles (CANPs) as potential nanosorbent for removal of Hg (II) ions *Environ. Nanotechnology, Monit. Manag.* **6** 32–44
[106] Shafiabadi M, Dashti A and Tayebi H A 2016 Removal of Hg (II) from aqueous solution using polypyrrole/SBA-15 nanocomposite: experimental and modeling *Synth. Met.* **212** 154–60
[107] Yao X, Wang H, Ma Z, Liu M, Zhao X and Jia D 2016 Adsorption of Hg(II) from aqueous solution using thiourea functionalized chelating fiber *Chinese J. Chem. Eng.* **24** 1344–52
[108] Saleh T A, Tuzen M and Sarı A 2018 Polyamide magnetic palygorskite for the simultaneous removal of Hg(II) and methyl mercury; with factorial design analysis *J. Environ. Manage.* **211** 323–33
[109] Bansal M, Ram B, Chauhan G S and Kaushik A 2018 L-Cysteine functionalized bagasse cellulose nanofibers for mercury(II) ions adsorption *Int. J. Biol. Macromol.* **112** 728–36
[110] Hamza M F, Wei Y, Benettayeb A, Wang X and Guibal E 2020 Efficient removal of uranium, cadmium and mercury from aqueous solutions using grafted hydrazide-micro-magnetite chitosan derivative *J. Mater. Sci.* **55** 4193–212
[111] Sun N, Wen X and Yan C 2018 Adsorption of mercury ions from wastewater aqueous solution by amide functionalized cellulose from sugarcane bagasse *Int. J. Biol. Macromol.* **108** 1199–206
[112] Tu H, Yu Y, Chen J, Shi X, Zhou J, Deng H and Du Y 2017 Highly cost-effective and high-strength hydrogels as dye adsorbents from natural polymers: chitosan and cellulose *Polym. Chem.* **8** 2913–21
[113] Bai L, Hu H, Zhang W, Fu J, Lu Z, Liu M, Jiang H, Zhang L, Chen Q and Tan P 2012 Amine/acid catalyzed synthesis of a new silica-aminomethyl pyridine material as a selective adsorbent of copper *J. Mater. Chem.* **22** 17293
[114] Wu F C, Tseng R L and Juang R S 2001 Kinetic modeling of liquid-phase adsorption of reactive dyes and metal ions on chitosan *Water Res.* **35** 613–8